

# ACTIVE CAMBER SYSTEM

*Vehicle System Dynamics*

**Professor:**

*Antonio Carcaterra*

**Members of Team 23:**

*Azhar Muhammedu - 1838818*

*Brighten Joseph - 1713116*

*Gupta Sandeep Kumar - 1844011*

*Sooraj Francis Mani - 1642365*

# Abstract

Conventional vehicles didn't reach their full potential because of the limitation in maneuverability. The main goal of the active camber concept to generate a vehicle with extreme maneuverability. The maneuverability of an automobile is limited by tire forces. While considering tire/road friction a significant portion of this friction is not utilized when tires steer. By adjusting camber, it is possible to generate up to 30% more lateral tire force. The result is a more maneuverable vehicle with increased turning capacity.

This study on Active camber system investigates the effects of cambering on overall vehicle stability by improving both lateral and rollover stability of conventional vehicles. A full vehicle model with change in camber is employed to investigate the vehicle dynamics. A linearized vehicle model is used to analytically study the effects of camber lateral forces on vehicle dynamics. The dynamic behavior of the vehicle for different configurations of camber angles and steering angles at various speed are analyzed. Then, an active camber system is implemented for the improvement of vehicle lateral stability. It was studied the variations of different lateral parameters like lateral velocity, yaw and roll angle were compared and analyzed by carrying out different simulations with individual effects of camber and steering, combined camber-steering, active camber and active steering. Also investigated and analyzed on, active front camber is more effective in improving maneuverability and lateral stability than active front steering.

**Keywords:** Active camber system, lateral stability control, Active steering system

# Contents

<b>1. Introduction.....</b>	<b>1</b>
<b>1.1 Vehicle Dynamics Concepts .....</b>	<b>3</b>
<b>1.1.1 Coordinate System .....</b>	<b>3</b>
<b>1.1.2 SLIP PARAMETERS .....</b>	<b>4</b>
<b>1.1.2.1 Sideslip angle.....</b>	<b>4</b>
<b>1.1.2.2 Slip angle .....</b>	<b>4</b>
<b>1.1.3 VEHICLE GENERAL CHARACTERISTICS.....</b>	<b>5</b>
<b>1.1.4 TIRE Theory.....</b>	<b>6</b>
<b>1.1.5 Active Camber System .....</b>	<b>7</b>
<b>1.1.5.1 Camber mechanism.....</b>	<b>7</b>
<b>1.1.5.2 Camber Angle .....</b>	<b>8</b>
<b>1.1.5.2.1 Effect of camber angle in tire characteristics.....</b>	<b>9</b>
<b>1.1.5.2.2 Camber angle and lateral forces .....</b>	<b>13</b>
<b>1.1.5.2.2.1 Camber contact patch.....</b>	<b>13</b>
<b>2. Methodology .....</b>	<b>15</b>
<b>2.1 Vehicle Model.....</b>	<b>15</b>
<b>2.2 Planar Motion.....</b>	<b>15</b>
<b>2.3 Roll Motion.....</b>	<b>17</b>
<b>2.4 Linear Model.....</b>	<b>18</b>
<b>2.5 Active Camber System .....</b>	<b>20</b>
<b>3. Simulation &amp; Results .....</b>	<b>21</b>
<b>3.1 ACTIVE CAMBER VS ACTIVE STEERING .....</b>	<b>31</b>
<b>4. CONCLUSION .....</b>	<b>34</b>
<b>Reference.....</b>	<b>35</b>
<b>Appendix.....</b>	<b>36</b>
<b>Appendix A: MatLAB Code for Active camber and Active Steering System.....</b>	<b>36</b>
<b>Appendix B: Eigen Values and Stability.....</b>	<b>39</b>
<b>Appendix C: Simulink Model.....</b>	<b>43</b>



# 1. Introduction

For better driving performance and vehicle's safety, forces at the tire-road contact contribution has major role. From various studies and papers, it was understood that the camber angle of the wheel substantially affects these forces and thereby the range of a vehicle's traction, which is of critical value especially in emergency and evasive maneuvers. There are various active-camber design concepts present to evaluate possible improvements on vehicle response. In that majority of those refer to open-loop maneuvers with the focus on vehicle response and therefore leave the driver out. but the driver is still responsible for the control of the vehicle so that driver's perception is critical to alter the control and response of the vehicle. The driver should understand the vehicle's response and the behavior after a steering input. Primarily, the influence of the wheel camber on the steering feel & overall control of the vehicle is investigated; which in turn redefines the safety experience. The vehicle model is modified to change and control the camber angle of the wheels. The driver can easily control / steer away the vehicle from the hazard by increasing the tire forces. Similarly, by decreasing the tire forces it is possible to change the stability of the vehicle & can prevent a roll-over or a spin.

Active control systems help to improve vehicle performance and safety and enhance their stability, handling, and comfort. Vehicle lateral stability control has been developed for preventing vehicle from spinning and drifting, also increasing vehicle maneuverability and safety. Active stability systems help the drivers in dangerous conditions like slippery road or aggressive maneuvering, to safely control the vehicle. Differential braking, torque vectoring, and active steering are well-known lateral stability systems. Currently, suspension systems with the capability of changing the camber angle are developed based on the idea of employing the cambering lateral forces. Camber means tilting the wheels relative to the vertical surface as viewed from front/rear. Camber angle leads to lateral force on the wheel known as camber thrust or camber force. Latest model suspension systems have an additional degree of freedom (DOF) for changing the camber angle to increase tire lateral forces and improve handling and stability of the vehicle.



Figure 1: 2002 Mercedes F400 Carving Concept

As an interesting study, an active camber system has been designed for Mercedes F400 Carving Concept in 2002. Camber system developed for this vehicle has the capability to increase lateral force and utilization of potential friction capacity by using a new technology. A specialized suspension system with special tires has been designed which can provide a cambering angle of 20° for outer wheels in a turn. This mechanism can able to increase the peak lateral force by 28%. An active camber system is also developed at Stanford University with the goal of increasing vehicle maneuverability.



Figure 2:Stanford's P1 steer-by-wire testbed at Altamont Raceway (left), Lotus super seven replica at thunder hill Raceway (right)

Based on their study, cambering can increase tire lateral force up to 30% thereby considerably enhancing turning capacity of the vehicles and making them more maneuverable. But for this, suitable tire needed for the change in camber. Conventional tires are not appropriate for large camber angles, the vehicles need to have specialized tires to achieve advantages of cambering. After deciding that, an active camber suspension system is developed. A prototype has also been constructed to validate the performance of the suspension system and different tires. Variable geometry suspension systems have also been considered for changing camber angle to enhance vehicle stability. The control system is responsible for enhanced vehicle performance in various situations considering yaw rate tracking, roll stability, and geometry limits.

An electronic camber suspension mechanism is proposed by Park and Sohn that can decrease the undesirable camber angle in conventional vehicles. It is shown that reducing unwanted camber angle improves the vehicle stability through the yaw rate response and lateral acceleration. This suspension system is designed by modifying a double wishbone type suspension and a control system is established using the bicycle model. Reduction in camber angle helps the vehicle with better cornering performance and enhanced lateral stability. Rear wheel camber control is also proposed to modify roll steer characteristics of the vehicles. This modification results in the increase of stability factor by about 11%. Optimization problem is defined and solved to obtain the best camber angles to take advantages of potential tire forces.

This study investigates cambering effects on entire vehicle's behavior and explores the capability of cambering for lateral stability improvement especially for urban vehicles. Urban vehicles have been introduced to deal with energy consumption, traffic problems, air pollution, and parking limitations in large cities. Basically, urban vehicles are smaller and narrower than conventional vehicles, by that cambering is potentially more effective for those vehicles. While limited studies have been conducted about active camber systems, this work investigates cambering effects on vehicles' behavior in detail & study of general equation that analytically shows cambering effects on overall vehicle dynamics behavior. This equation compares cambering effects with steering effects and is applicable to different vehicles in linear zone of tire forces. So, with the help of an active camber system it is possible to improve lateral stability of the vehicle. It is shown how this active camber system compares with the active front steering. More specifically, the contributions of this study can be listed as follows: 1. Application of active camber systems to urban vehicles for lateral stability improvement; 2. Analytical study of camber effects on overall vehicle dynamics behavior.

## 1.1 Vehicle Dynamics Concepts

### 1.1.1 Coordinate System

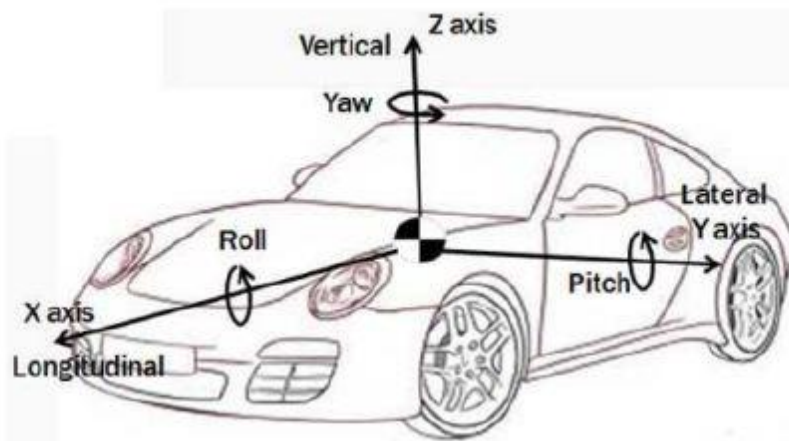


Figure 3: Vehicle Coordinate System

For simulating vehicle dynamics, the vehicle is simplified to a single point in space, with a given mass  $m$  at the center of gravity (CoG) and a moment of inertia  $I$ . The CoG moves along three dimensions in space which are described using a coordinate system. As an automotive standard  $x$  is defined as the forward direction of the vehicle. The positive  $y$  direction is to the left side of the vehicle (looking from the top). The positive  $z$  direction is to the top side of the vehicle. Besides

the three transversal movements, the vehicle rotates along the three axes. Rotation around the  $x$ -axis is referred to rolling and is determined by the angle. Rotation around the  $y$ -axis is known as pitch angle. Rotation around the vertical  $z$ -axis is defined as yaw angle.

## 1.1.2 SLIP PARAMETERS

### 1.1.2.1 Sideslip angle

In vehicle dynamics there are three defined slip quantities to study the vehicle behavior. The first is the side-slip angle,  $\beta$ . This is the angle between the vector velocity and the  $x$  axis of the vehicle coordinate system.

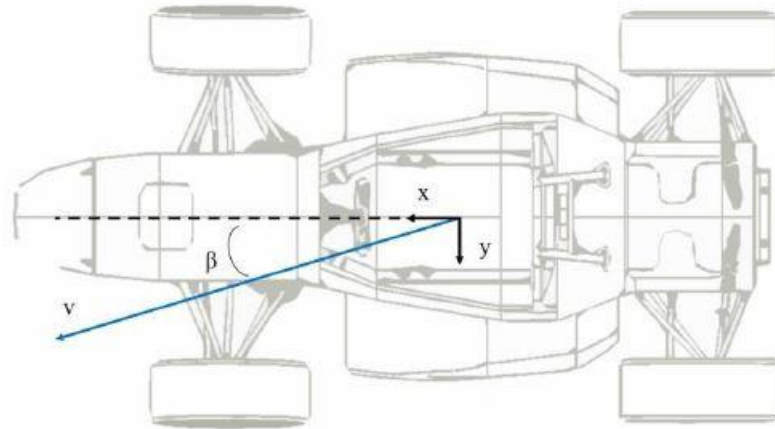


Figure 4: Sideslip Angle Representation

The other slip quantities are important in tire dynamics and their influence in force generation in the contact patch will be explained later. As of now, they will be presented as they are defined.

### 1.1.2.2 Slip angle

The first slip quantity is the Slip Angle, SA. This is the angle measured between the direction in which the wheel is heading and the direction of the velocity of that wheel projected onto the  $x_{ty}$  plane (Figure 5). It represents a measure of the distortion that generates or is generated by lateral force in the tire contact patch.

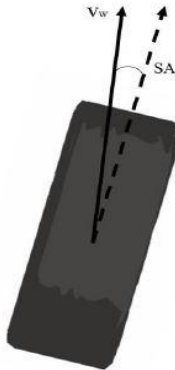


Figure 5: Tire Slip angle Representation

### 1.1.3 VEHICLE GENERAL CHARACTERISTICS

There are some general dimensions and weight properties that can be said as being a vehicle characteristic and not of some specific area of the vehicle. In the following table the ones of most importance for this work is presented.

**Table 2.** Vehicle's parameters.

Parameters	Values	Descriptions
$m$	800 kg	Vehicle mass
$m_s$	680 kg	Sprung mass
$a$	1.25 m	Distance of front wheels to CG
$b$	1.25 m	Distance of rear wheel to CG
$I_x$	$210 \text{ kg m}^2$	Roll inertia
$I_z$	$480 \text{ kg m}^2$	Yaw inertia
$H$	0.5 m	CG height
$h_s$	0.4 m	Distance of CG from roll center
$T$	1.4 m	Vehicle track
$k_\varphi$	11,760 N/rad	Torsional stiffness
$c_\varphi$	784 N s/rad	Torsional damping
$R$	0.3 m	Wheel radius
$K_R$	0.5	The front-to-rear ratio of total lateral load transfer

CG: center of gravity.

### 1.1.4 TIRE Theory

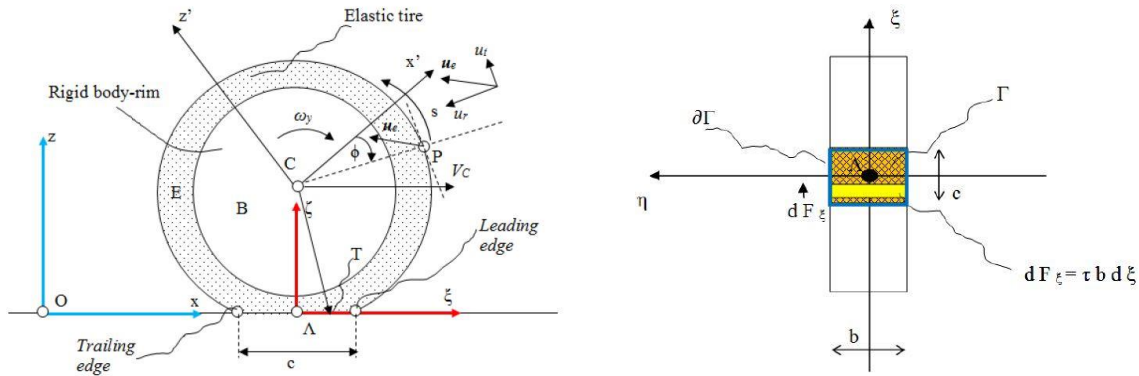


Figure 6: Scheme of the elastic tire and the tire-road contact (left), Top view scheme of the tire-road contact (right)

The tires are vital components for vehicle modeling since tires transmit forces from the ground to the vehicle and vice versa. By using general and simplified kinematics we can introduce a simplified model of the elastic wheel, based on a simple elastic behavior. In local elastic model it assumes that if a force is applied at the point P on the outer surface of E, the elastic response displacement of E remains confined to P and its response is instantaneous or static. In any real elastic system, like the tire, when loaded by a point force produces an elastic displacement that involves the entire system E. If one is loading the tire at one single point P on its surface, it can see that the circle shape of the tire deformed over an entire region about P. Considering that the region about P, interested in the deformation produced by the load, is generally small. Moreover, under certain conditions discussed later, and neglecting the dynamic inertial effects, this hypothesis is reasonable at least for small rolling speeds. An image for this elastic model, but nothing more than a visualization, consists simply in assimilating E to a set of massless elastic bristles, attached by an elastic clamp to B that can be bent generating both tangential and radial forces. In figure 1, a sketch of the model is presented. The contact of the wheel with the road covers a surface  $\Gamma$ , a rectangle (a simplifying hypothesis) of length  $c$  and width  $b$ , the footprint (see figures 1 and 2). The first segment along the footprint that the tire particles meet during the wheel rolling is the leading edge, the last segment of the footprint they touch before leaving the road plane is the trailing edge (see figure 1). The bristles or brush elements are, in the present simple model, elastically clamped over the rigid body B (the rim), while the rod-beam element and an elastic foundation, will be included later in the BRB model (Brush-Rod-Beam model). Three reference systems are introduced: the road-coordinate system  $R(O, x, y, z)$ , integral to the road plane, and of unit vectors  $i, j, k$ , the wheel coordinate system  $W(C, x', y', z')$ , integral with the rigid B-part of the wheel, and the reference system  $G(\Lambda, \xi, \eta, \zeta)$  following the flat tire-road contact region  $\Gamma$ . Namely, G has the  $\xi$  axis that is the intersection of the road plane with the mid-plane of the rim (the rigid part of the wheel) passing through its center C,  $\zeta$  normal to the road-plane and pointing in the opposite direction with respect to the ground,  $\eta$  axis lying on the road-plane

normal to  $\xi$ . The origin  $\Lambda$  is the point of intersection between the plane passing through C and orthogonal to the  $\xi$  axis, and the  $\xi$  axis itself

### 1.1.5 Active Camber System

In order to improve the stability of the vehicles, the concept of wheel cambering is investigated as a new technology. In addition to the idea of increasing lateral force and improving lateral stability, the capability of cambering in rollover stability of narrow vehicles is also studied.

#### 1.1.5.1 Camber mechanism

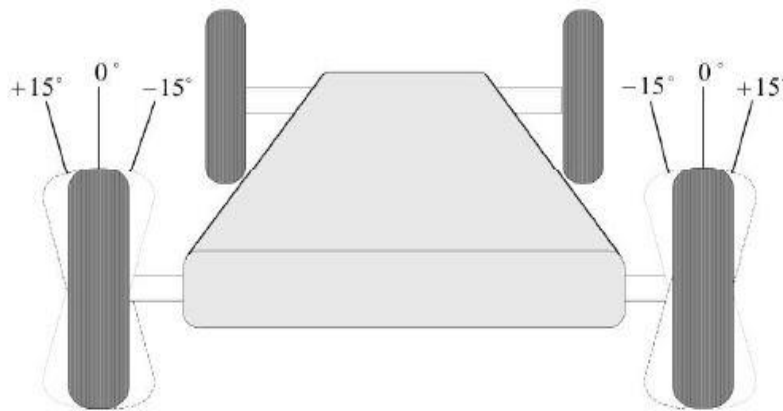


Figure 7: Wheels Cambering

Camber is the tilt of the wheels relative to the vertical surface as viewed from front or rear (Figure 7). The tire that tilts outward at the top is defined to have a positive camber angle and the tire with inward tilt at the top is defined to have a negative one as shown in Figure 7. Camber angle leads to lateral force on the wheel known as camber thrust or camber force. Normally for the conventional suspension system vehicles, small predetermined amount of positive or negative camber angles are applied as they are designed to improve handling and steering of the vehicle; but these small camber angles are not variable. Because of these non-varying camber angles, this kind of cambering is not desirable and can degrade the handling properties.

Recently, the suspension systems with the capability of purposefully changing the camber angle are developed based on the idea of employing the cambering lateral force. The new suspension systems have additional degree of freedom for changing the camber angle in order to improve handling and stability of the vehicle. As an interesting research project, an active camber system is developed at Stanford University with the goal of increasing vehicle maneuverability. Based on the research project of active camber system developed by Stanford University, by cambering it is possible to increase tire lateral force up to 30% thereby considerably enhancing turning capacity of the vehicles and making them more maneuverable. Their first part of the study is

based on tires because conventional tires are not suitable for this camber change. And in the second part, an active camber suspension system is developed. A prototype has also been constructed to validate the performance of the suspension system and different tires.

In another study, a variable geometry suspension system is designed to recognize camber change for improvement of vehicle stability. This suspension system is controlled with a robust control system that automatically changes the camber angles of the rear wheels. The control system is responsible for enhanced vehicle performance in various situations considering roll stability and geometry limits. Also, an electronic camber suspension mechanism is proposed that can decrease the undesirable camber angle in conventional vehicles. It is shown that reducing unwanted camber angle improves the vehicle stability including yaw rate and lateral acceleration. As another research project, a system is introduced to modify roll steer characteristics of the vehicle by controlling rear wheel camber. By this modification, stability factor increases for about 11%. It is a simple mechanism so that it is easily implemented. The purpose of these research in camber angle is to show the capability of this new technology for increasing lateral force and utilization of potential friction capacity. By a special suspension system with special tires F400 can provide a cambering angle of 20 degrees for outer wheels in a turn. It is shown that this mechanism can increase the peak lateral force by 28%.

### 1.1.5.2 Camber Angle

A camber angle changes characteristics of a vehicle, also its dynamic behavior. Specifically, camber affects tire lateral forces, vehicle track, and vehicle's CG height. To find out the influence of active camber on the steering feel it is important to understand what the effect of camber is. The camber angle is the angle of the tire around its X-axis, shown in Figure 8 (like a motorcycle leaning into the corner). In the SAE standard the camber angle is defined as "the angle between the wheel and the vehicle body, while the inclination angle is the angle between wheel and perpendicular to the road".

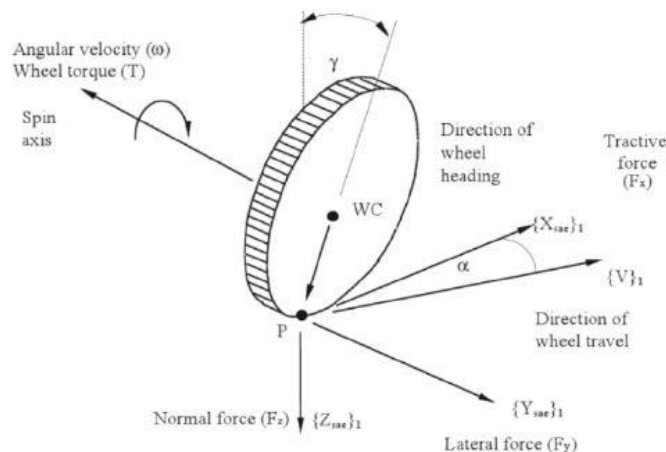


Figure 8: Tire Axis Frame, SAE Standard

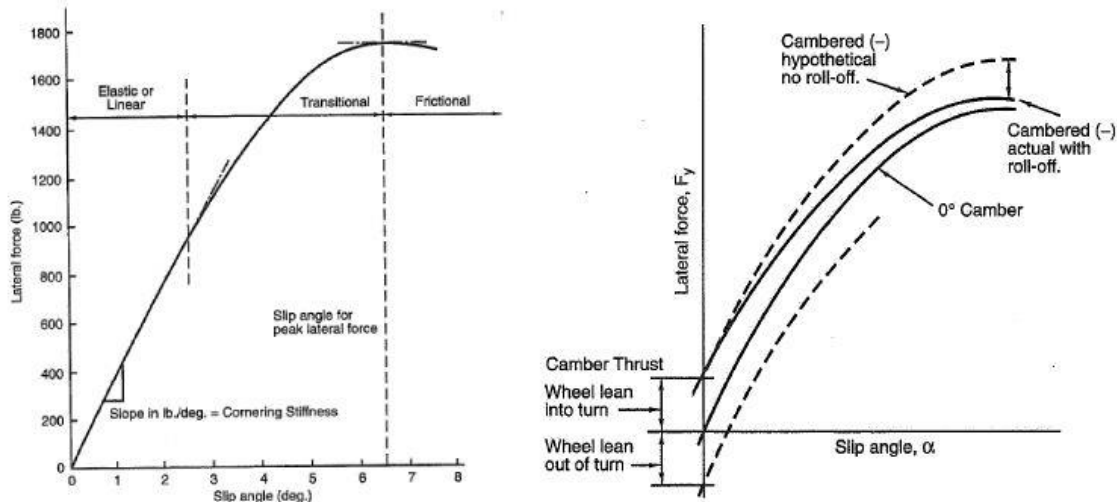


Figure 9: The lateral force tire characteristics. First the linear elastic part, then a transition to the peak force and finally a frictional part where the slip angle is too large and the lateral forces decreases(left), The Camber thrust (right), when leaning the curve into the corner, lateral force increases.

The sign of the camber angles is mirrored on the vehicle, because a negative camber angle is when the wheel is leaning inwards the vehicle, while a positive camber angle is when the wheel is leaning outwards the vehicle. This means if the tires are leaning into the corner a positive camber angle is used for the inner corner wheels, while a negative camber is used for the outer corner wheels.

#### 1.1.5.2.1 Effect of camber angle in tire characteristics

From the figure 9 at first The lateral force increasing linear with slip angle, after reaching a specified slip angle its linearity is lost and reaches its maximum lateral force. After that when the slip angle increases the lateral forces decreases. The lateral force can be shifted by changing the camber angle of the tire. In the corner, a higher lateral tire force can be produced, when leaning out of the corner it decreases the lateral tire force. This is called camber thrust. The reason for this camber thrust is due to tire properties like stiffness, shape, material use, etc.

If the linear range exceeds the additive effects of camber inclination decreases. This effect is called the roll-off which is also shown in Figure 9. This is a characteristic due to the shape of the tire and the combination of camber angle and slip angle. The contact area of the tire is called the tire print. The deformation of the tire print leads to the generation of the lateral tire forces. To gain a better understanding of the tire print distortion during cornering as shown in figure 10. During cornering the angle of steer change the orientation with respect to the road. At the front side of the tire print the tire comes in contact and sticks to the road. When rotating the wheel, the tire is pushed sideways due to the inertia of the vehicle body and the tire starts deforming. These increase in deformation of the wheel lasts till the vertical force decreases and the tire wants to get back to its original plane of the tire. From this point to the end of the print the tire slides and the distortion decreases again. This distortion is the displacement  $u$  in Hooke's law ( $F$

$\Delta \epsilon_{ik} \propto u$ ) and therefore, the distortion pattern is equal to the lateral force distribution as shown in Figure 11.

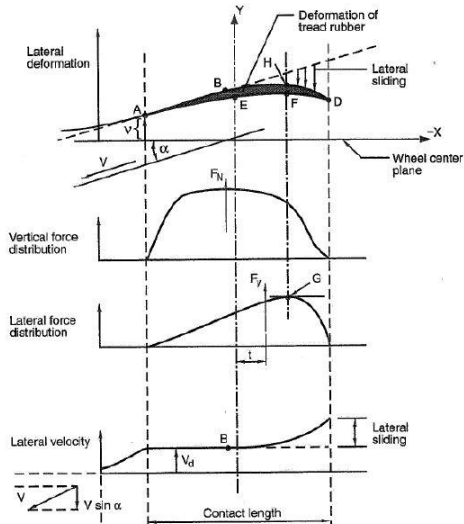


Figure 10: The tire print deformation, distribution of the forces and lateral velocity over the contact length. This fig. shows the development of the tire forces on a schematic view for a corner to right. The vehicle is turned to the right with angle  $\alpha$ , but the vehicle velocity is still out of the corner. In point A the tire meets the road and sticks to the road as the wheel turns. Due to the inertia of the vehicle the tire deforms, and point A follows the velocity line to point B, where the wheel center is shifted to point E. Thus, the tire sticks to the road and follows path ABHD and the wheel center follows path AEFD. therefore, the deformation and the thus the force increases over the contact length. Finally, the resultant force of the lateral tire forces is positioned after the wheel center with distance t, which leads to the aligning torque of the wheel.

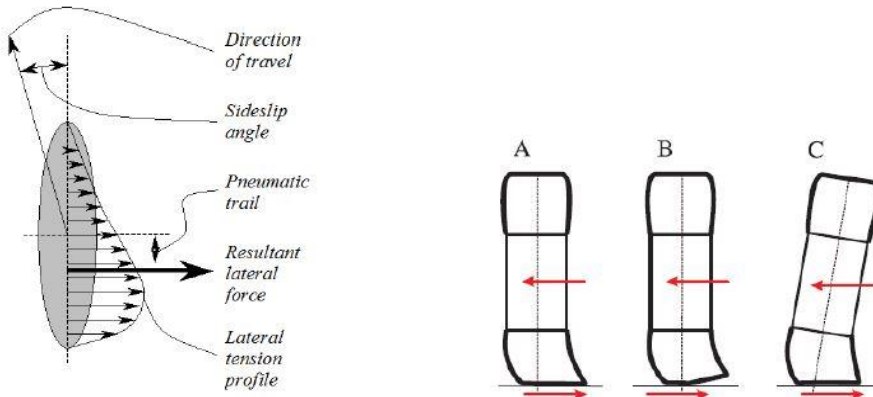


Figure 11: Tire deformation pattern due to slip (left), Tire deformation during cornering (right), (A) – Tire deforms due to lateral forces, (B) – In extreme cases this leads to extreme deformation & the contact area decreases, (C) - When tilting the tire into the corner the contact area recovered

Using camber angle creates an almost symmetric tire print, because the plane of the tire is parallel to the plane of the tire sticking to the road and there is almost no development of slip angle. But in order to make a corner, camber angle is not enough, so that a combination of slip angle and camber angle is used. By adding camber angle, distortion pattern changes and shifts the resultant lateral force towards the center of the tire. The distance from the resultant lateral force to the tire center is the pneumatic trail and has influence on the aligning torque.

A large moment will be created in the neutral camber position of the wheel due to the applied lateral forces, while the resultant forces of a negative tilted wheel will be mostly loaded in axial direction. Due to this property, tire is less depended on the cornering stiffness of the wheel in tilted orientation. For a small tire with low cornering stiffness, the camber angle will increase the contact area due to the deformation as shown in Figure 11. In "A" the tire is deformed due to lateral force, but "B" shows what happens due to the lateral force. In "C" a re-establishment of the contact area is done by tilting the tire. But for a wider tire with high cornering stiffness, a large camber angle will result in a lower contact area, due to its stiff square cross-section. Therefore, researchers design and use rounded cross-section tires. This design allows maintaining an enough contact area on the road surface while tilting the tire. The shape and stiffness are also very important properties for the tire design of a camber actuated suspension system.

The tire contact area is essential for the tire forces, because the friction coefficient of the tire is load sensitive. That means lower load is more efficient than a higher load, which leads to wide tires. A wider tire distributes the load over the tire but also has a higher friction coefficient. So that, it is useful to aim for the largest possible tire contact area. The normalized lateral force with respect to the vertical load is presented for a race tire in Figure 12. The tire with lower load reaches a higher normalized lateral force, which means a higher lateral force per load. The contact area also has a major role in tire wear, temperature, pressure and other features indirectly related to the tire. Even though the contact area increases the lateral force, but it also increases the factors like tire wear, temperature etc.

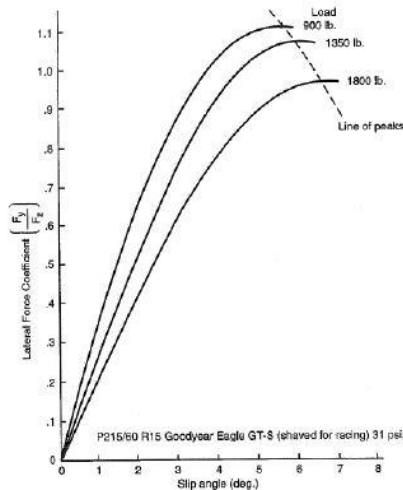


Figure 12: The normalized lateral force with different loads, This graph shows that a better load distribution over the tires can improve the lateral force coefficient for this race tire.

A longitudinal slip related to longitudinal forces, and a lateral slip or slip-angle related to lateral forces and moments are two slip definitions for tires. Figure 13 shows the combined slip of longitudinal traction and lateral force. An important feature to note is the decrease of lateral force during braking or accelerating. The shape of the circle will depend on tire because for a wide race tire the diagram is larger and more elliptical, so it reaches higher lateral forces.

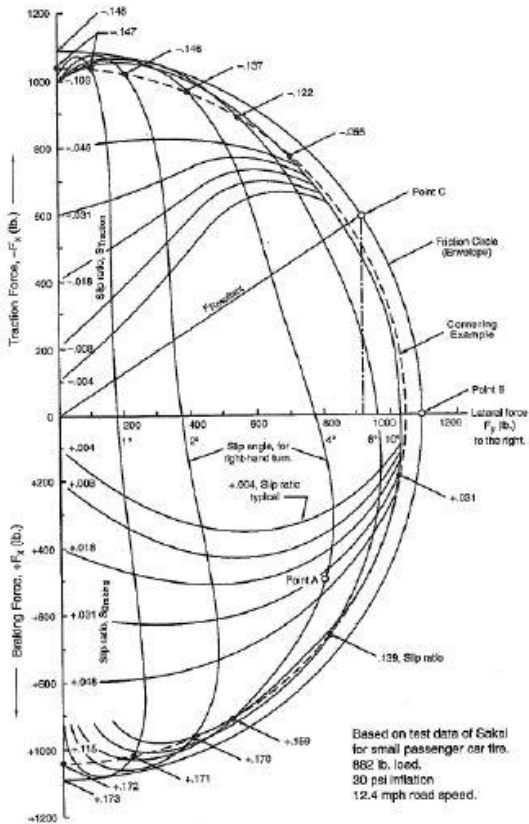


Figure 13: The friction circle for a small passenger car tire, when accelerating or braking during cornering results in combined slip in the tires. This leads to a decrease in lateral and longitudinal forces.

Camber angle can change the friction circle. There are multiple tire models available with their own method of simulating the responses and these are classified as analytical and empirical models in general. One of the empirical models is the Magic tire formula. It has 20-100 coefficients and can be extended to over 300 coefficients. Where the coefficients represent the stiffnesses, compliances and many more tire properties. There are multiple studies showing that the lateral vehicle dynamics can be improved with larger camber angles. These studies show that a larger camber angle can increase the lateral forces, the lateral acceleration and the yaw rate.

### 1.1.5.2.2 Camber angle and lateral forces

#### 1.1.5.2.2.1 Camber contact patch

The tire lateral forces in conventional cars arise from sideslip angles. Applying a steering angle on a vehicle results in the sideslip angle and, which leads to lateral forces on both front and rear wheels. The maximum tire lateral force is limited by friction force between the tire and road. But when lateral forces generated only by sideslip angle, a significant portion of maximum lateral force cannot be used efficiently. Introducing the Camber is another way to generate the lateral force with the capability to increase the maximum lateral force for vehicles. The tire contact patch during cambering is totally different from that of sideslip angle. Similarly, the friction force is utilized in a different way. Figure 14 shows a simple one-dimensional (1D) tire brush model for sideslip angle and camber. The deformation in tire contact patch, caused by sideslip angle, has a triangular shape as demonstrated in Figure 14(a). The contact patch deformation in cambering has an arc shape as shown in Figure 14(b).

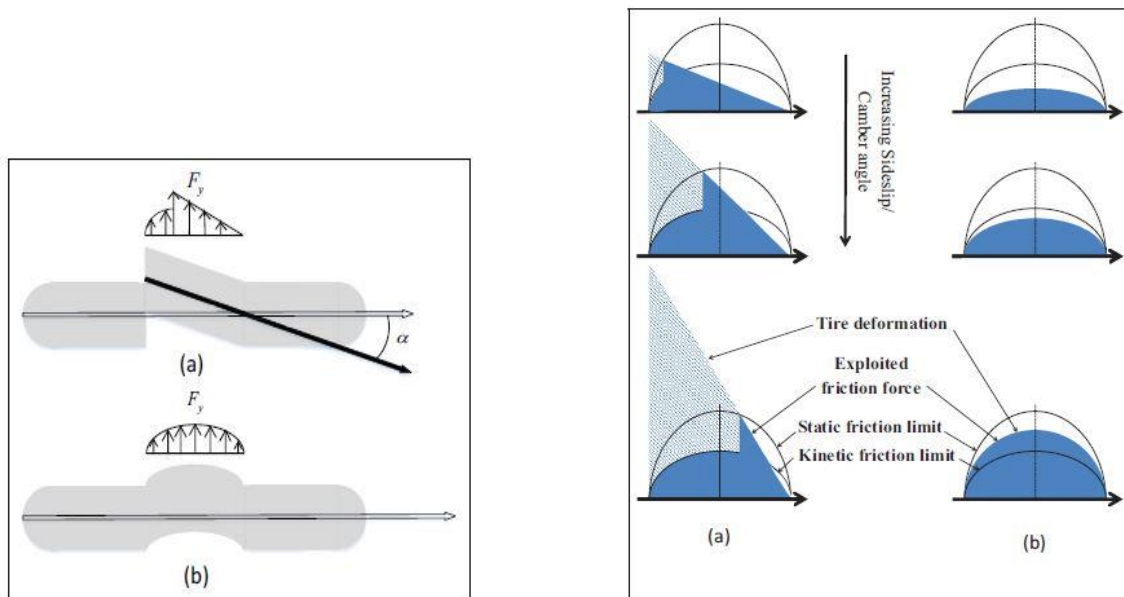


Figure 14: Left - Tire contact patch for lateral force creation (a) sideslip angle (b) Camber Angle, Right - Friction utilization to general lateral forces (a) side slip angle & (b) camber Angle

The friction in the contact patch depends on the vertical force distributed at the contact patch. The limitation for the resulting static and kinetic friction forces are illustrated in Figure 14. When static friction limit is exceeded, the tire begins to slide; since the friction force in sliding is less than that in adhesion, the tire lateral force decreases when sliding occurs. For a triangular shape

of contact patch in sideslip angle, always some parts of the contact patch exceed adhesion and begin to slide as illustrated in Figure 14 right(a). Thus, most of the available friction will not be used. The part of the contact patch, that has sliding, increases for greater sideslip angles. In contrast, the arc shape of contact patch deformation in cambering has a closer match to the available static friction as shown in Figure 14 right(b). Almost all parts of the contact patch remain in adhesion zone for a large range of camber angles. As a result, more portions of friction capacity can be utilized by switching from sideslip to camber for lateral force generation. It is shown that camber has the potential to increase the lateral forces by up to 30%.

## 2. Methodology

### 2.1 Vehicle Model

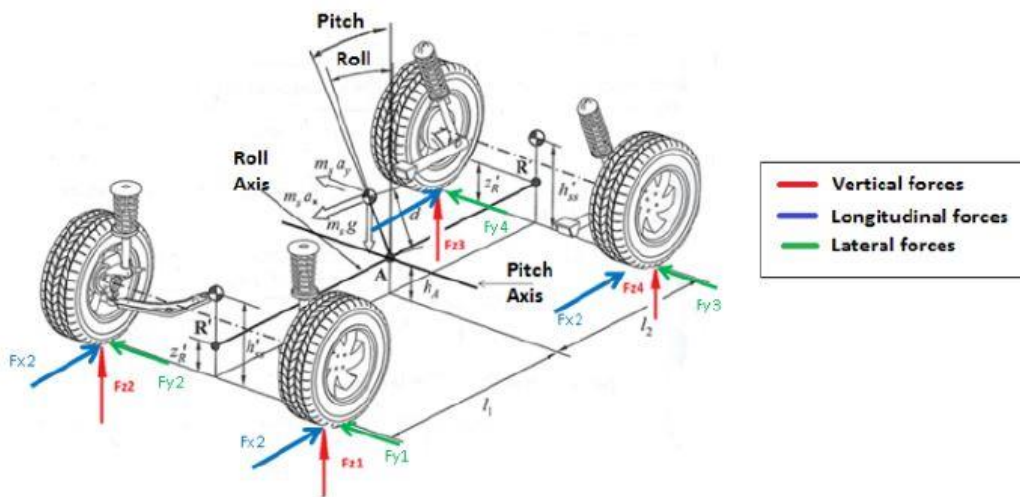


Figure 2. 1: Vehicle model

### 2.2 Planar Motion

A vehicle model with 3 DOF is used to examine the effects of cambering on vehicle lateral stability including lateral motion, yaw motion, and roll motion (Figure 2.2). Longitudinal velocity is assumed to be constant. This 3DOF model represents the basic characteristics of lateral stability responses. Let  $v$ ,  $u$ ,  $r$ , and  $\phi$  denote the lateral velocity, longitudinal velocity, yaw rate, and roll angle, respectively. The vehicle's body equations are as follows

$$m(\dot{v} + ur) + m_s h_s \ddot{\phi} = F_{y1} + F_{y2} + F_{y3} + F_{y4} \quad \dots (1)$$

$$I_z \ddot{r} = a(F_{y1} + F_{y2}) - b(F_{y3} + F_{y4}) \quad \dots (2)$$

- $v$  = Lateral velocity
- $r$  = Yaw
- $m_s$  = sprung mass
- $h_s$  = distance from roll center to cg
- $\varphi$  = roll angle
- $a$  = distance from cg to front wheel axle
- $b$  = distance from cg to rear wheel axle
- $\delta$  = steering angle
- $\alpha$  = slip angle
- $I_z$  = yaw moment of inertia

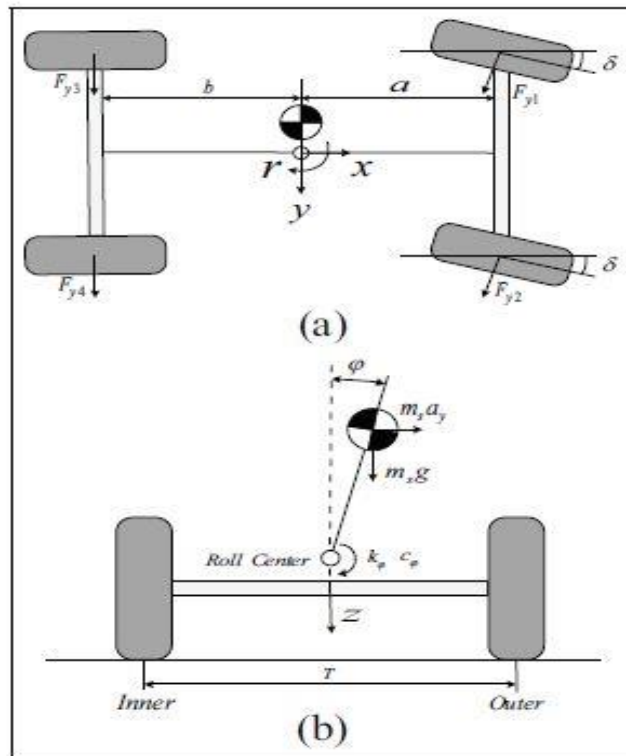


Figure 2.2: 3 DOF vehicle Model (top view)

The distances of the center of gravity (CG) from front wheels and rear wheels are denoted by  $a$ ,  $b$ .  $k_\varphi$  and  $c_\varphi$  represent the effective torsional stiffness and torsional damping for roll motion, and  $h_s$  denotes the distance of the CG from the roll center. Note that the wheels are denoted by numbers. Specifically, wheels 1–4 are the front-left, front-right, rear-left, and rear-right wheels, respectively.  $F_{yi}$  ( $i = 1 \dots 4$ ) represents the lateral force for wheel number  $i$ .

- $m(\dot{v} + ur) =$  centrifugal force acting on the vehicle
- $F_{y1}, F_{y2}, F_{y3}, F_{y4}$  are lateral forces generated on the wheels
- $F_{yi} = C_{\alpha i}\alpha_i + C_{\gamma i}\gamma_i$
- $C_{\alpha i}\alpha_i$  = lateral force due to slip angle (steer)
- $C_{\gamma i}\gamma_i$  = lateral force due to camber angle
- $\gamma_i$  and  $\alpha_i$  are camber and slip angles of the wheel
- $i = 1, 2, 3, 4$  (linear tire model)

$$\alpha_1 = \alpha_2 = \delta - (v + ar)/u$$

$$\alpha_3 = \alpha_4 = -(v - br)/u$$

## 2.3 Roll Motion

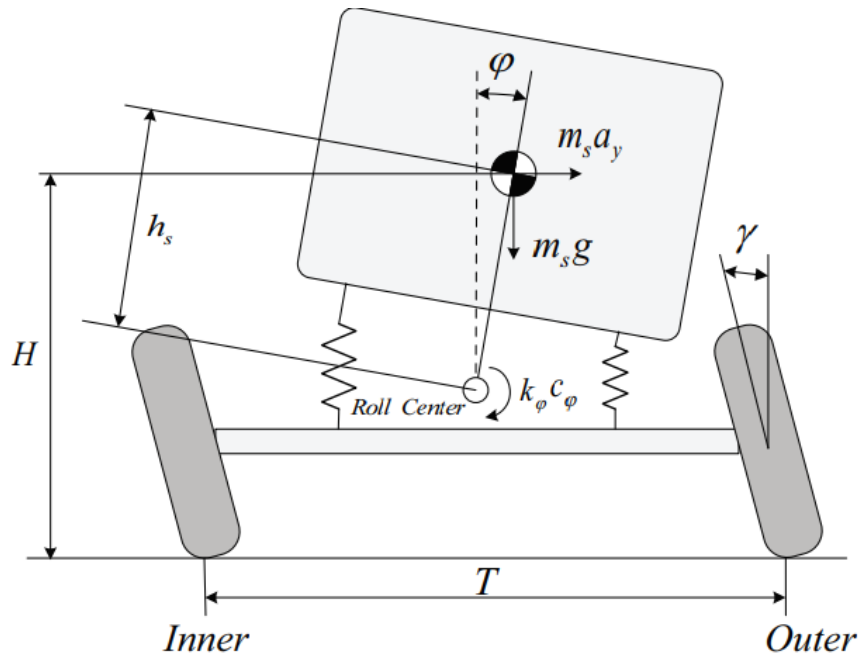


Figure 2. 3: Three DOF Vehicle Model (Front view)

When vehicle takes a curve, weight of the vehicle is thrown to the outside of the corner. If the speed of the vehicle is more than average, chances of roll over increases. These roll motion or tendency of roll is not a good factor while considering dynamics/stability of the vehicle. These roll over can be easily reduced with the help of change in camber angle. To study this phenomenon, we derive the equation of roll motion as follows:

$$I_x \ddot{\phi} + m_s h_s (\dot{v} + u r) + C_\phi \dot{\phi} + k_\phi \phi + m_s h_s g = 0 \quad \dots (3)$$

- $I_x$ =roll moment of inertia
- $C_\phi$ =damping coefficient (combined effect)
- $k_\phi$ = spring stiffness (combined effect)
- $g= 9.81 \text{ m/s}^2$

After the formation of these three equations, steering block were formed according to Ackermann steering condition ( $\cot \delta_i = (w/L) + \cot \delta_0$ ) on Simulink and numerous simulations were conducted at different condition like Camber angle, steering only & camber - steering combined, Active camber etc.

## 2.4 Linear Model

To investigate the effects of camber lateral forces on vehicle dynamics behavior and to design a controller, by linearizing the previous model  $v = r = \phi = \dot{\phi} = 0$ . The linear equations are rewritten as follows

$$m(\dot{v} + u r) + m_s h_s \dot{\phi} = F_{y1} + F_{y2} + F_{y3} + F_{y4}$$

$$I_z \ddot{r} = a(F_{y1} + F_{y2}) - b(F_{y3} + F_{y4})$$

$$I_x \ddot{\phi} + m_s h_s (\dot{v} + u r) + C_\phi \dot{\phi} + k_\phi \phi + m_s h_s g = 0$$

To obtain linear lateral tire forces it was assuming the steering and sideslip angle are very small. By these assumptions, the linear model for the tires including camber effects is written as follows

$$F_{yi} = C_{\alpha i} \alpha_i + C_{\gamma i} \gamma_i \quad \text{for } i = 1 - 4$$

Where  $C_{\alpha i}$ ,  $\alpha_i$ ,  $C_{\gamma i}$  &  $\gamma_i$  (for  $i=1_4$ ) represent cornering coefficient, camber coefficient, sideslip angle, and camber angle for tire  $i$ . Positive and negative camber angles are defined differently from those in conventional suspension systems. Here, the camber angle is calculated independently for each wheel about XYZ axis attached to the body of the vehicle. Similar values of camber angles mean that the wheels are parallel. The front and rear sideslip angles can be written as follows

$$\alpha_1 = \alpha_2 = \delta_f - (v + ar)/u$$

$$\alpha_3 = \alpha_4 = -(v - br)/u$$

where  $\delta_f$  denotes the front steering applied by the driver, and  $\delta_1 = \delta_2 = \delta_f$ . In this study, the steering input for each wheel is separately modelled to compare the effects of cambering and steering of each single wheel. Substitution of the sideslip angle equations and in the lateral tire force equation, and then substituting in the vehicle model and rewriting in state-space form, the linear vehicle model is obtained as follows

$$\dot{X} = AX + B\delta + E\gamma \quad X = [v \ r \ \phi \ \dot{\phi}]^T \quad \delta = [\delta_1 \ \delta_2]^T \quad \gamma = [\gamma_1 \ \gamma_2 \ \gamma_3 \ \gamma_4]^T$$

$$B' = \begin{pmatrix} C_{\alpha 1} & C_{\alpha 2} \\ \frac{m+n}{I_z} & \frac{m+n}{I_z} \\ \frac{aC_{\alpha 1}}{I_z} & \frac{aC_{\alpha 2}}{I_z} \\ 0 & 0 \\ \frac{-m_s h_s C_{\alpha 1}}{(m+n) I_x} & \frac{-m_s h_s C_{\alpha 2}}{(m+n) I_x} \end{pmatrix} \quad E = \begin{pmatrix} C_{\gamma 1} & C_{\gamma 2} & C_{\gamma 3} & C_{\gamma 4} \\ \frac{m+n}{I_z} & \frac{m+n}{I_z} & \frac{m+n}{I_z} & \frac{m+n}{I_z} \\ \frac{ac_{\gamma 1}}{I_z} & \frac{ac_{\gamma 2}}{I_z} & \frac{-bc_{\gamma 3}}{I_z} & \frac{-bc_{\gamma 4}}{I_z} \\ 0 & 0 & 0 & 0 \\ \frac{-m_s h_s c_{\gamma 1}}{I_x(m+n)} & \frac{-m_s h_s c_{\gamma 2}}{I_x(m+n)} & \frac{-m_s h_s c_{\gamma 3}}{I_x(m+n)} & \frac{-m_s h_s c_{\gamma 4}}{I_x(m+n)} \end{pmatrix}$$

$$A = \begin{pmatrix} a_{11} = \frac{-(2c_{af} + c_{ar})}{\left(\frac{-m^2_x h^2 s}{I_x} + m\right)u} & a_{12} = \frac{\left(\frac{-m^2 s h^2 s u^2}{I_x} + mu^2 + 2ac_{af} - bc_{ar}\right)}{\left(\frac{-m^2 x h^2 s}{I_x} + m\right)u} & a_{13} = \frac{\frac{-m^2 s h^2 s g}{I_x} + \frac{m_s h_s k_\varphi}{I_x}}{\left(\frac{-m^2 s h^2 s}{I_x} + m\right)} & a_{14} = \frac{\frac{m_s h_s c_\varphi}{I_x}}{\left(\frac{-m^2 s h^2 s}{I_x} + m\right)} \\ a_{21} = \frac{-(2c_{af} - bc_{ar})}{uI_z} & a_{22} = \frac{-(2a^2 c_{af} + b^2 c_{ar})}{uI_z} & a_{23} = 0 & a_{24} = 0 \\ a_{31} = 0 & a_{32} = 0 & a_{33} = 0 & a_{34} = 1 \\ a_{41} = \frac{2c_{af} m_s h_s + c_{ar} m_s h_s}{\left(\frac{-m^2 s h^2 s}{I_x} + m\right)u} & a_{42} = \frac{2ac_{af} m_s h_s - bar m_s h_s}{\left(\frac{-m^2 s h^2 s}{I_x} + m\right)u} & a_{43} = \frac{-m k_\varphi - mg m_s h_s}{\left(\frac{-m^2 s h^2 s}{I_x} + m\right)u} & a_{44} = \frac{\frac{m c_\varphi}{I_x}}{\left(\frac{-m^2 s h^2 s}{I_x} + m\right)} \end{pmatrix}$$

## 2.5 Active Camber System

In this section, an active camber system is provided for lateral stability control of an urban vehicle. The linear vehicle model is employed and a linear-quadratic regulator (LQR) controller is developed assuming front and rear camber systems as the actuators. LQR is selected over PID controller. Because LQR controller can able to respond faster than PID & also LQR control method has better performance as compared to PID. The performance index of the optimal controller is defined as follows

$$J = \frac{1}{2} \int_0^{\infty} [(X_d - X)^T Q (X_d - X) + U^T R U] dt$$

where  $X_d$  and  $U$  represent desired response and control input, respectively;  $Q$  and  $R$  are the weighting matrices. The optimal control input to minimize this performance index is given by

$$U = -R^{-1} E^T (P X + S)$$

where  $P$  and  $S$  are the controller parameters. For a constant steering input and infinite time, by ignoring the transient part of the solution,  $P$  and  $S$  will be obtained from the following algebraic equations

$$A^T P + P A - P E R^{-1} E^T P + Q = 0$$

$$(A^T - P E R^{-1} E^T) S - Q X_d + P B \delta_f = 0$$

The control law has the state feedback term and the feed-forward term. The control input can be rewritten as follows

$$U = K_v v + K_r r + K_\phi \dot{\varphi} + K_{\dot{\phi}} \dot{\phi} + K_\delta \delta_f$$

where  $K_v$ ,  $K_r$ ,  $K_\phi$ ,  $K_{\dot{\phi}}$  &  $K_\delta$  represent control gains for lateral velocity, yaw rate, roll angle, roll rate, and driver steering command. The desired values for the states are  $X_d = [0, r_d, 0, 0]^T$ , where  $r_d$  is the desired yaw response obtained from the following equation

$$\frac{r_d}{\delta_f} = \frac{u}{l + k_{usd} u^2}$$

where  $l$  is the wheelbase and  $k_{usd}$  is the desired understeer coefficient for the vehicle. In general, the understeer coefficient is an important criterion to evaluate handling characteristics of vehicles and describes the sensitivity of vehicles to the steering input.

### 3. Simulation & Results

#### 3.1 Behavior of lateral velocity generated during

1. Camber only
2. Steering and camber-steering combined
3. Active camber

Observations from figure 3.1(camber only):

- maximum lateral velocity of the vehicle is generated when the longitudinal velocity and camber are maximum
- lateral velocity increases with an increase in both longitudinal velocity and camber angle
- when camber is kept constant lateral velocity changes with respect to longitudinal velocity and vice versa
- Also, a linear relationship between the variables can be observed initially and lateral velocity settles to a constant value later

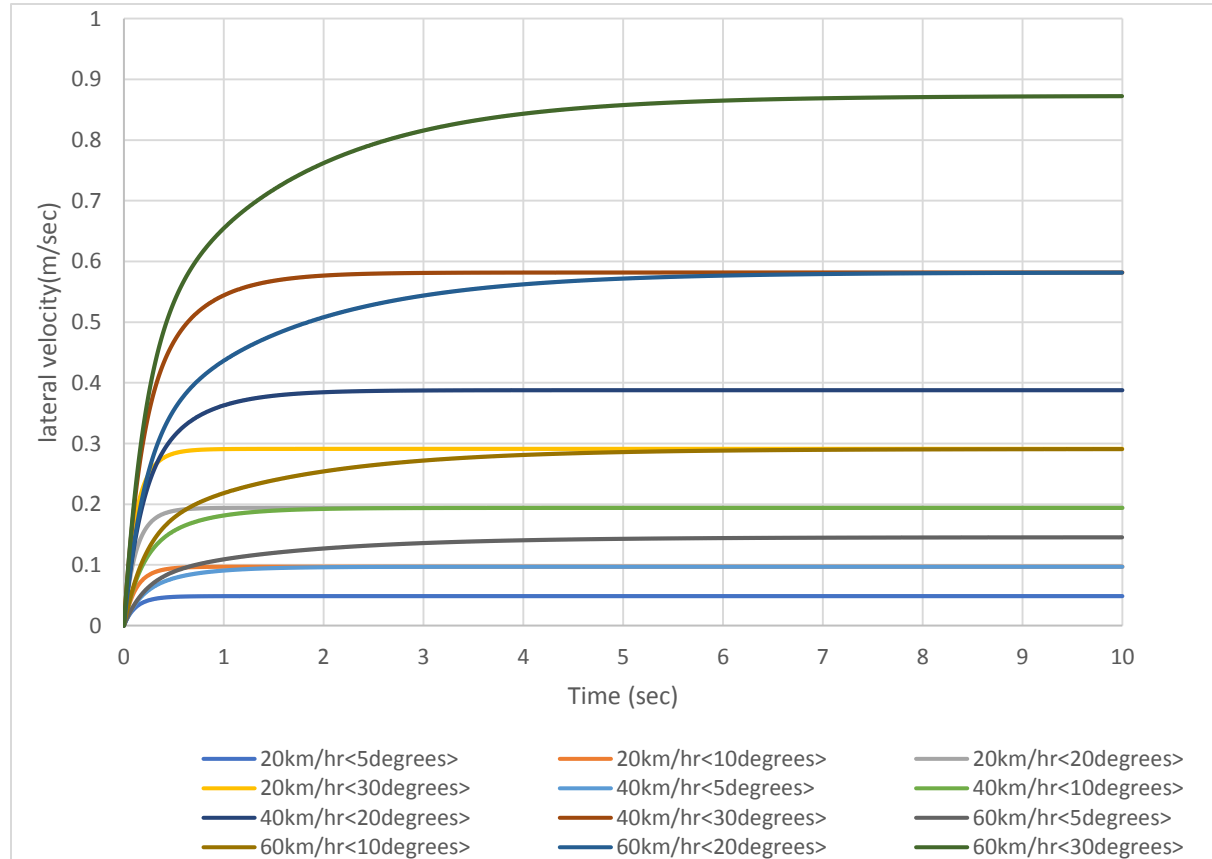


Figure 3.1: This graph shows the variation of lateral velocities of the vehicle for a time period of 10 sec at longitudinal velocities of 20,40 and 60 Km/hr at four different camber angles of 5,10,20 and 30°.

Observations from figure 3.2a and 3.2 b (steering and camber-steering combined):

- When steering alone condition is considered lateral velocity is maximum for higher steering angle
- There is an undesirable generation of lateral force at steering only condition before it is later stabilized (fig 3.4b)
- But in case of combined steering-camber condition the transition is smooth (fig 3.4b)
- When longitudinal velocity increases, steering gain also increases compared to the previous case, but the transition is smoother in combined case

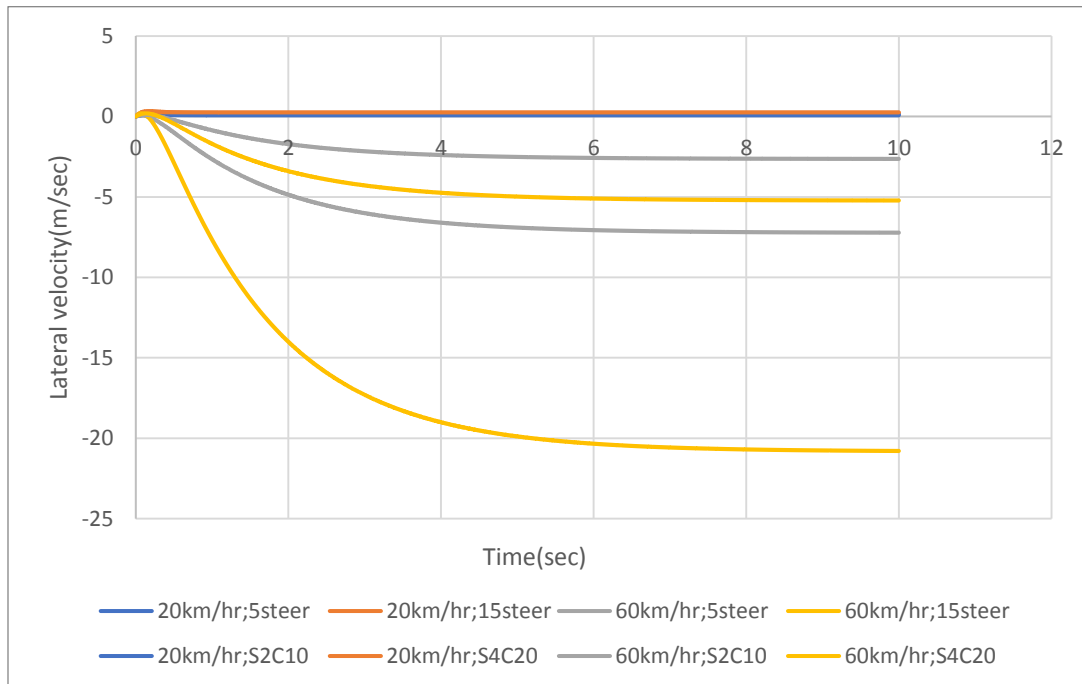


Fig 3.2a: Variation of lateral velocities of the vehicle for a time period of 10 sec at longitudinal velocities of 20 and 60 Km/hr for steering angle alone and combined steering-camber

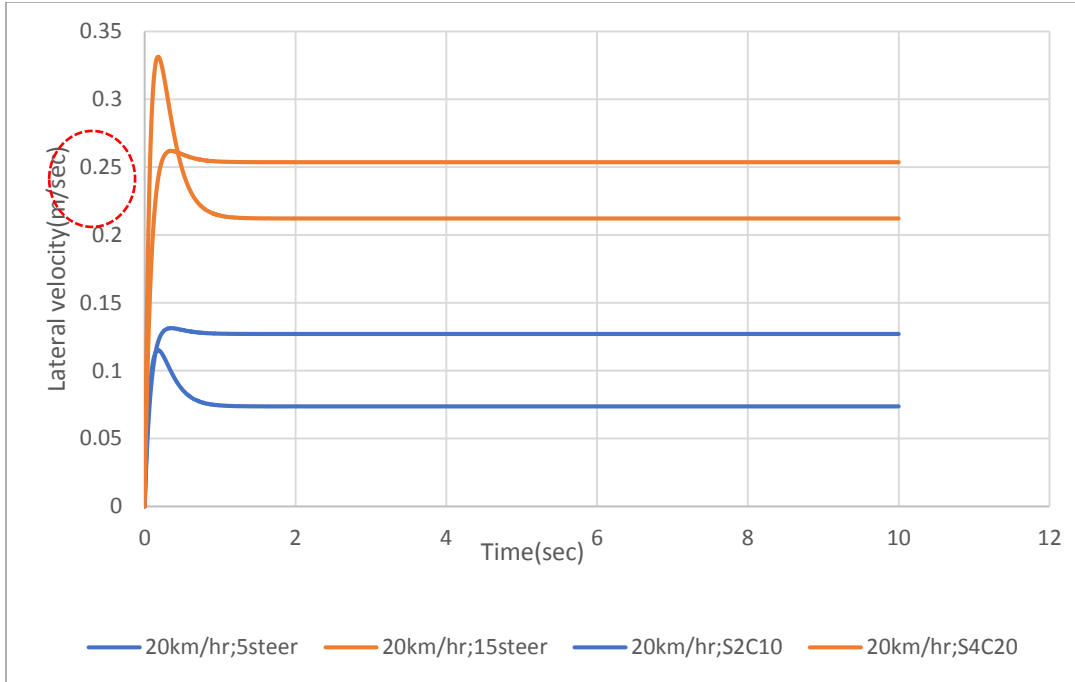


Fig 3.2b: behavior of lateral velocity at 20 km/h for steering only and camber-steering combined

#### Observations from figure 3.3(active camber):

- there is an initial linear relationship between lateral velocities and time for all the cases considered but after certain duration of time lateral velocity becomes constant
- lateral velocity generated is more at higher yaw
- maximum lateral velocity generated in all the cases is almost at the same instance.

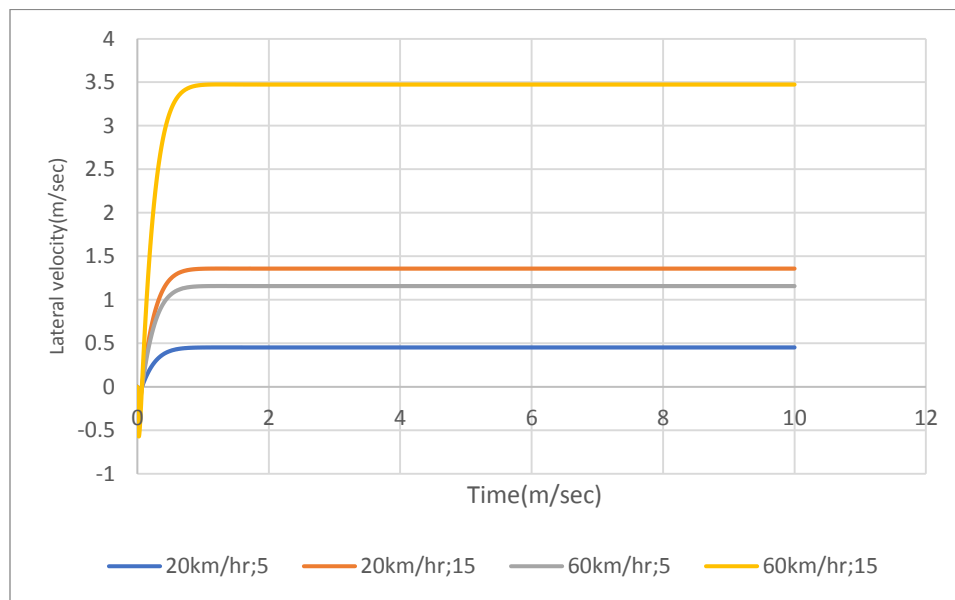


Fig3.3: variation of Lateral velocity during active camber for desired yaw generated from equivalent 5°steering and 15°steering with .001 understeer coefficient at 20 and 60 kmph.

The response to the input is much quicker in active camber condition compared to the previous cases, also lateral velocity get stabilized in shorter time period.

### **3.1 Behavior of yaw generated during**

- 1. Camber only**
- 2. Steering and camber-steering combined**
- 3. Active camber**

Observations from figure 3.4(camber only):

- yaw initially decreases exponentially to reach zero and later increases and settles down to zero
- the minimum value of yaw for each velocity is when the camber angle is maximum
- drop in yaw values is sharper at lower velocities

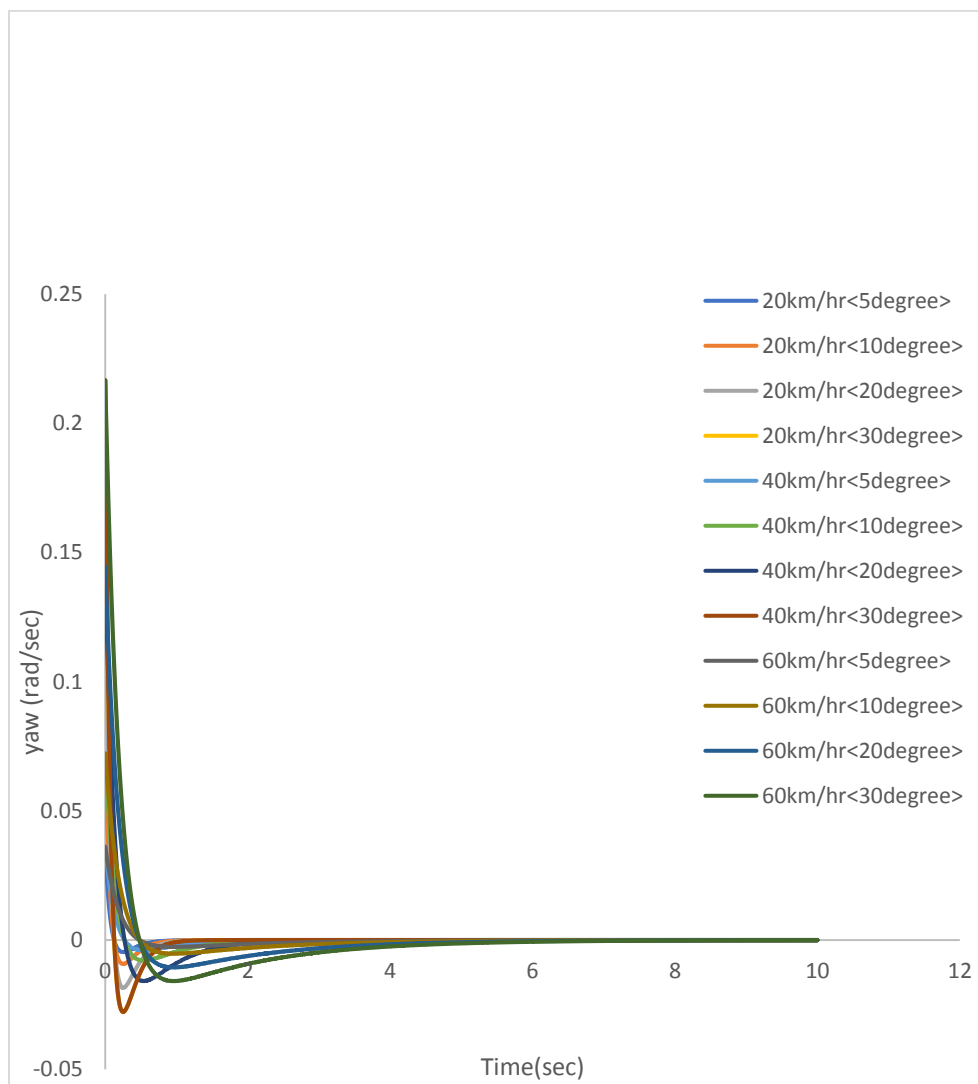


Fig 3.4: This graph shows the variation of yaw of the vehicle for a time period of 10 sec at longitudinal velocities of 20,40 and 60 Km/hr at four different camber angles of 5,10,20 and 30°.

Observations from figure 3.5 (steering and camber-steering):

- there is an instantaneous spike in yaw initially during this condition
- the drop of yaw to zero is faster at lower velocity
- the effect of yaw is dominant in steering only condition.

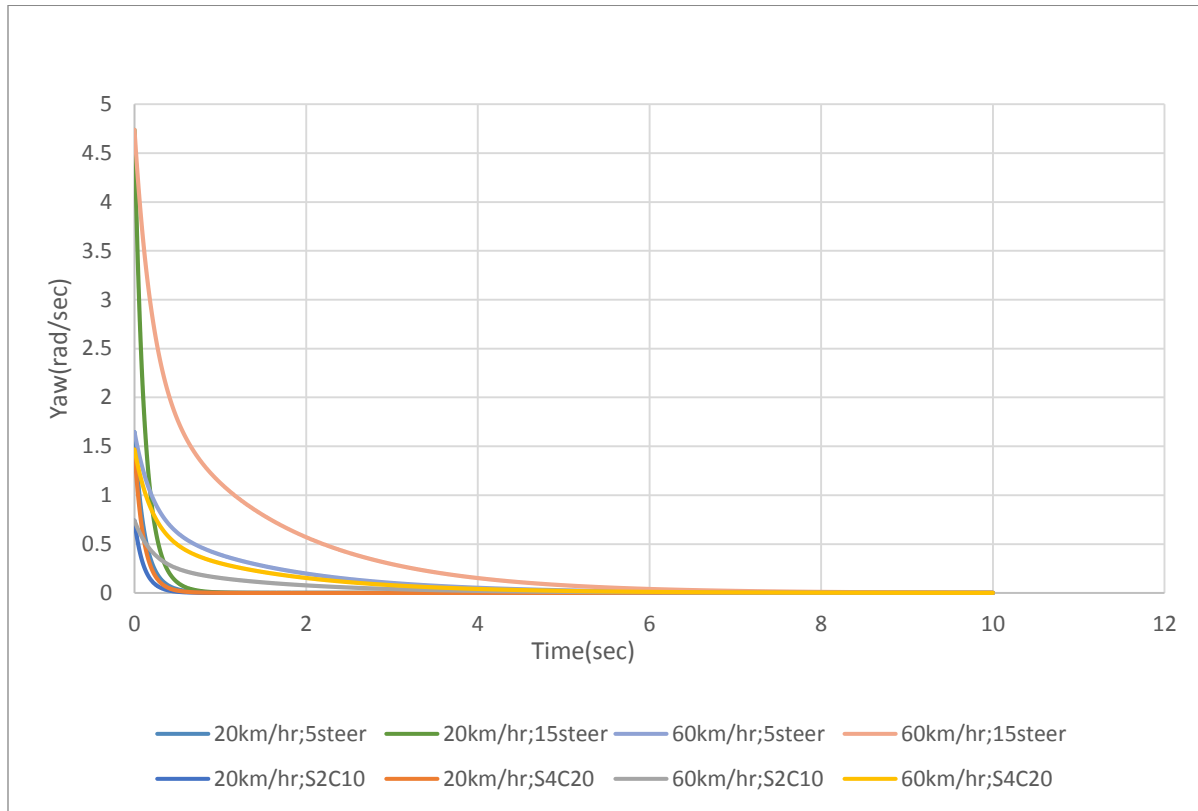


Fig 3.5: Variation of yaw of the vehicle for a time period of 10 sec at longitudinal velocities of 20 and 60km/hr for steering angle alone and combined steering-camber

Observations from figure 3.6(active camber):

- In case where yaw is higher it can be observed that the system response is quicker
- For all the different velocities considered the system tends to be stable at almost the same instance
- Initial intensity of yaw is maximum when velocity is maximum

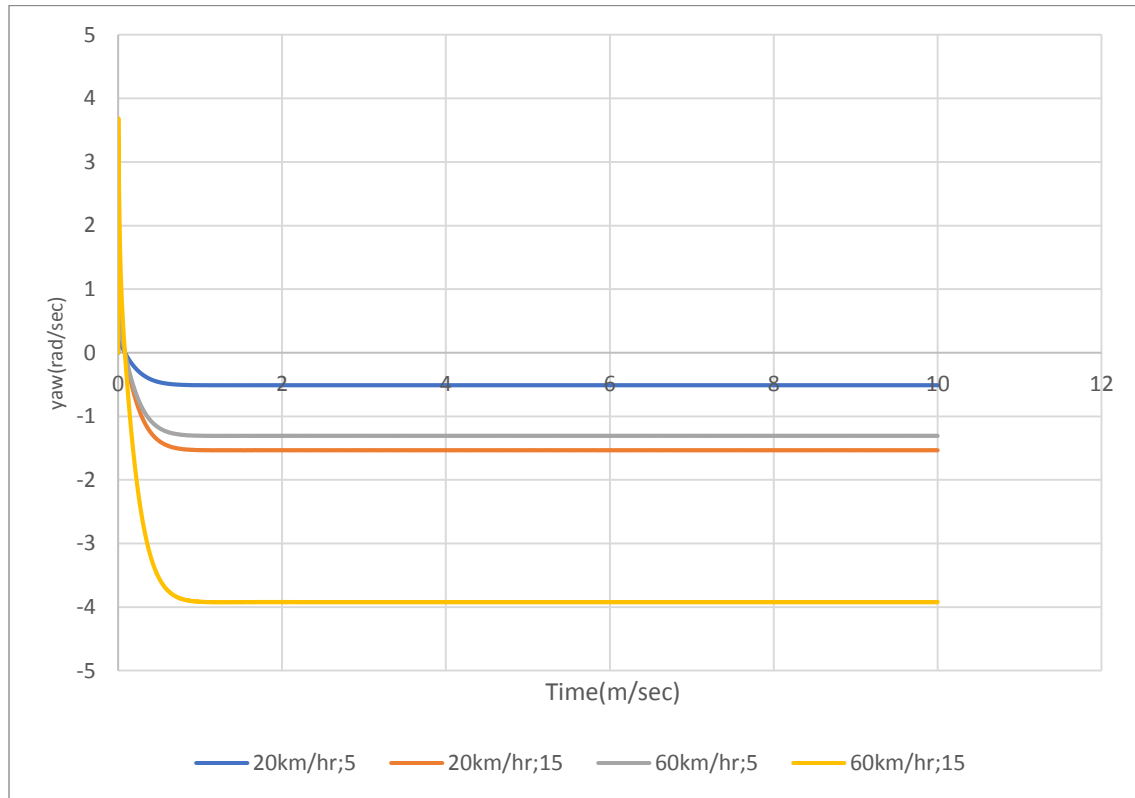


Fig3.6: variation of Yaw during active camber for desired yaw generated from equivalent 5-degree steering and 15° steering with .001 understeer coefficient at 20 and 60 kmph.

**Observations from figure 3.7(camber only):**

- The roll angle oscillates with respect to time for different velocities and camber angles
- Amplitude of oscillation is maximum when camber angle is maximum
- Frequency of oscillation is almost same at same longitudinal velocity
- Maximum roll angle is for the maximum velocity

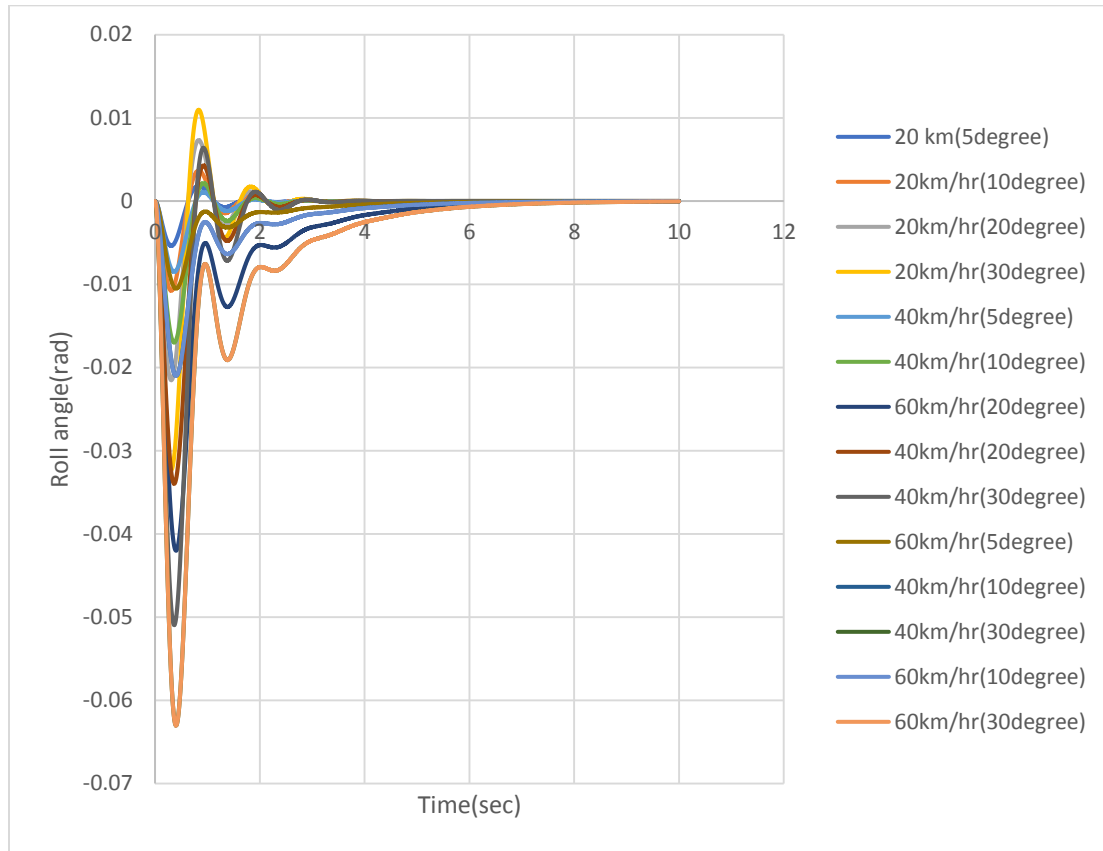


Fig 3.7: This graph shows the variation of roll angle of the vehicle for a time period of 10 sec at longitudinal velocities of 20,40 and 60 Km/hr at four different camber angles of 5,10,20 and 30°.

**Observations from figure 3.8(steering only and camber-steering):**

- All the roll angle tends to diverge from zero as time progresses reaches their maximum and remains constant
- At lower speeds an oscillation of roll angle is present for both steering only and camber-steering condition
- Amplitude of oscillation is observed to be higher steering only condition. However, the frequency is almost constant

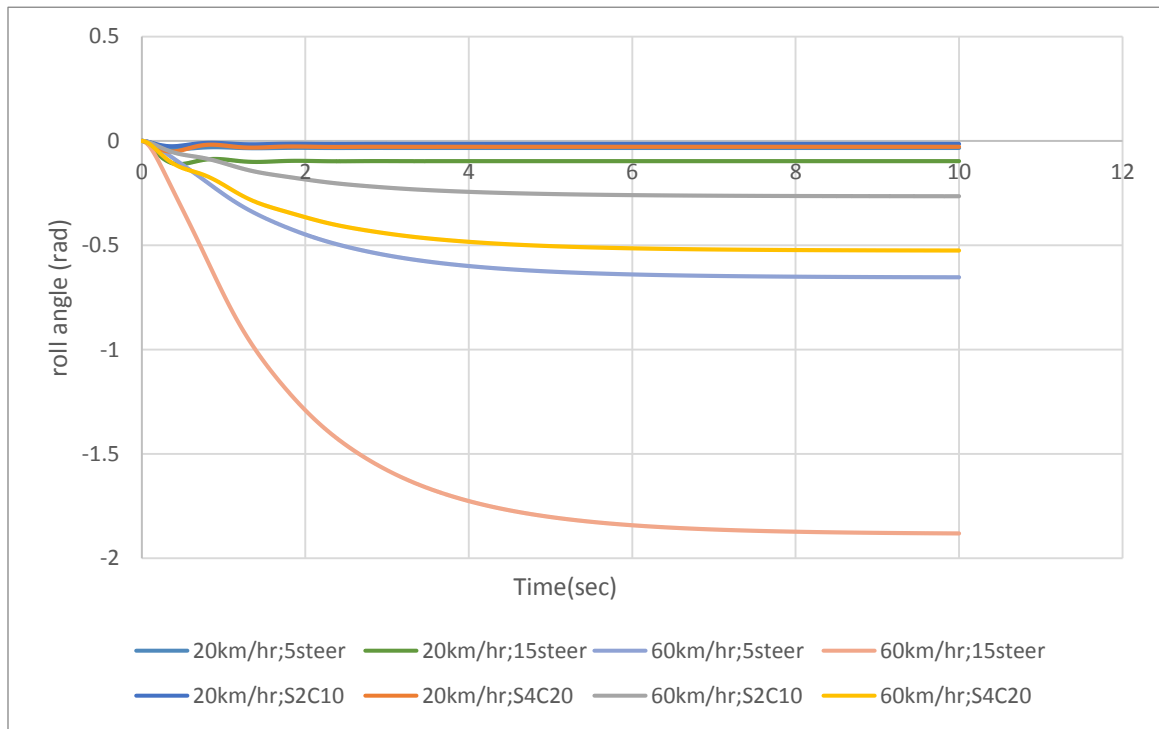


Fig 3.8: Variation of roll angle of the vehicle for a time period of 10 sec at longitudinal velocities of 20 and 60 Km/hr for steering angle alone and combined steering-camber

**Observations from figure 3.9:**

- At lower velocity the effect of roll is minimal
- Even though there is an initial peak in lower velocity it quickly stabilizes
- When velocity increases roll angle also increases but stabilizes after some time
- At higher velocities the curve is linear for some time before it reaches a constant value

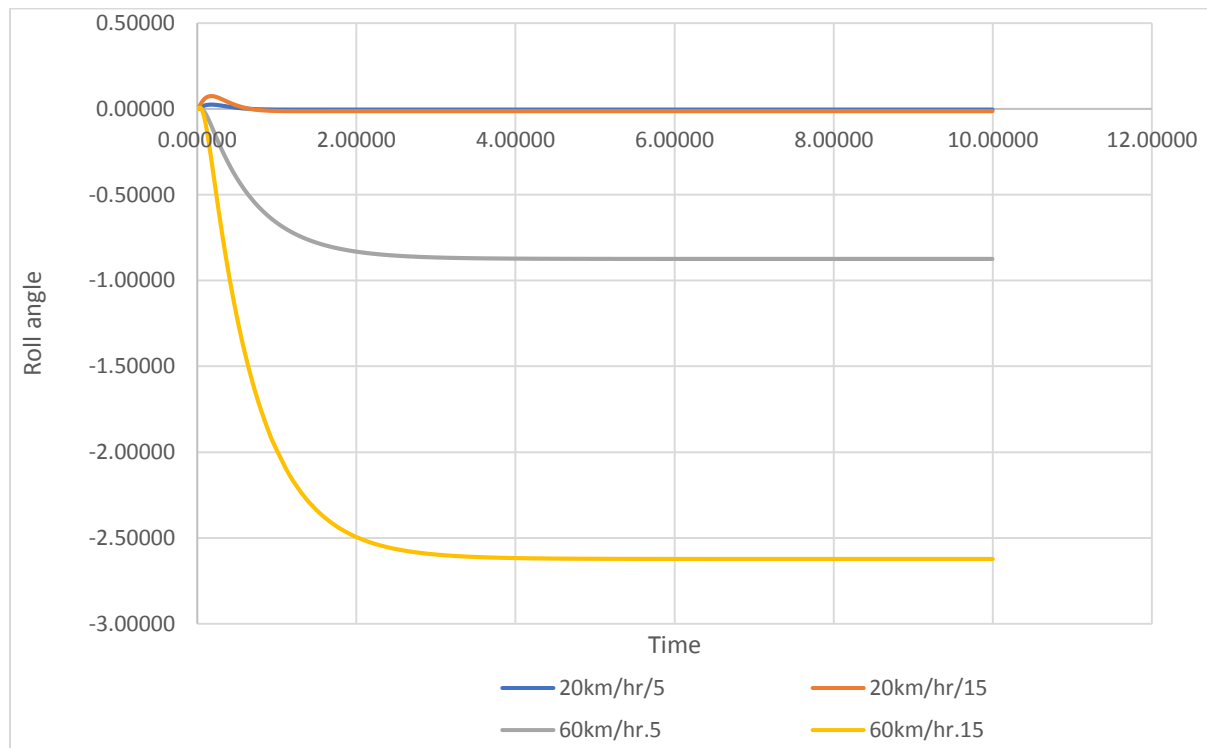


Fig3.9: variation of roll during active camber for desired yaw generated from equivalent 5° steering and 15° steering with .001 understeer coefficient at 20 and 60 kmph

### 3.1 ACTIVE CAMBER VS ACTIVE STEERING

Eventhough both active camber and active steering gave satisfactory results we did a comparison between the two to find out the best condition

#### Observations from fig 3.10(active camber vs active steering)

- Maximum lateral velocity is generated at higher longitudinal velocity for active camber
- But at lower longitudinal velocities active steering influenced lateral velocity more
- Time taken for lateral velocity to achieve a stable value is less for active camber

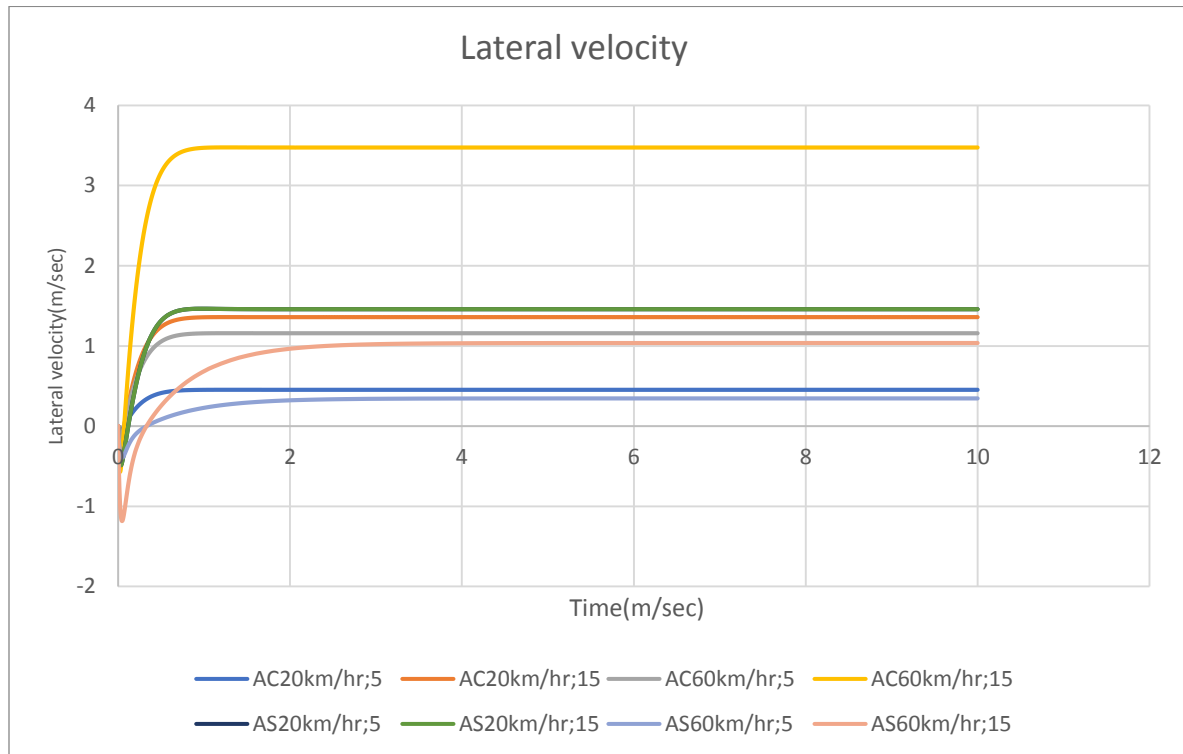


Fig 3.10: variation of Lateral velocity during active camber vs active steer for desired yaw generated from equivalent 5°steering and 15°steering with .001 understeer coefficient 20 and 60 kmph

### Observations from fig 3.11(active camber vs active steering)

- Maximum yaw is generated at higher longitudinal velocity for active camber
- But at yaw velocities active steering influenced lateral velocity more
- Yaw value settles to a constant value quicker in case of active camber

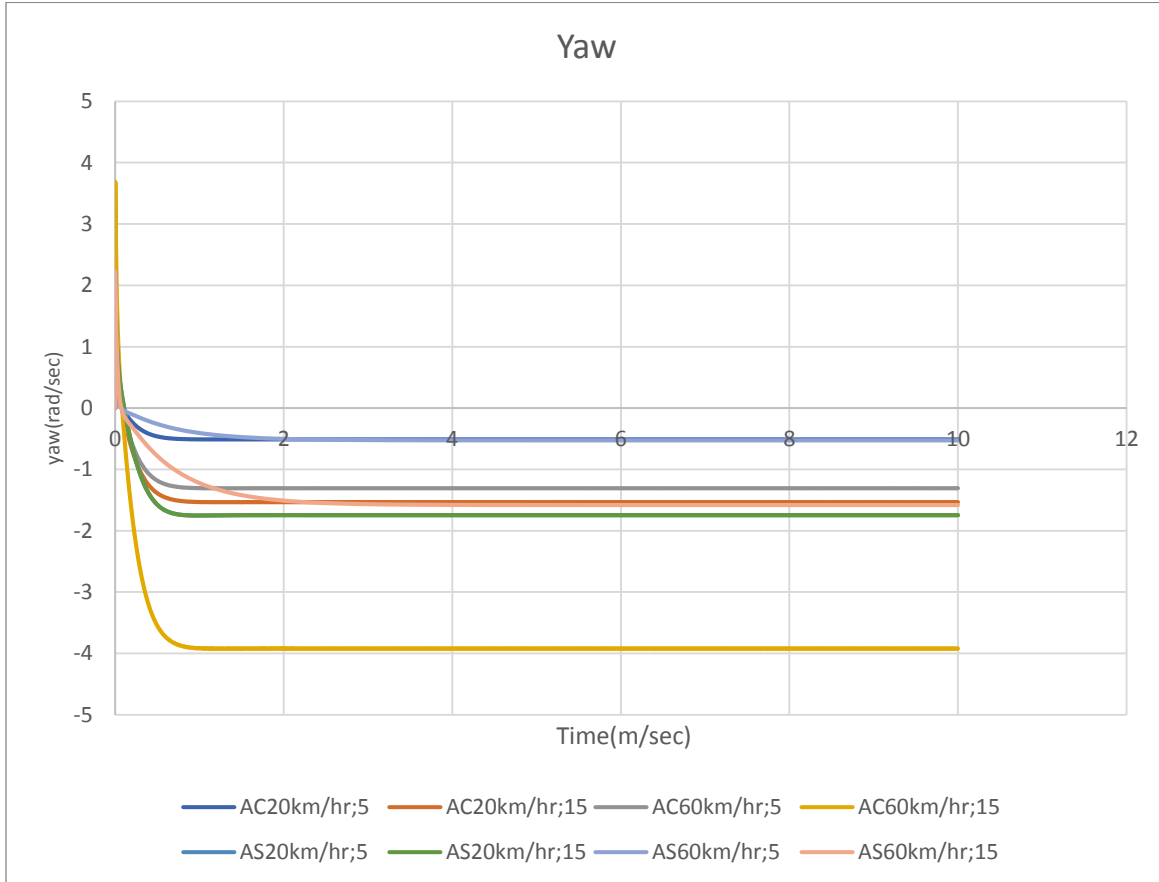


Fig 3.11 : variation of yaw during active camber vs active steer for desired yaw generated from equivalent 5° steering and 15° steering with .001 understeer coefficient at 20 and 60 kmph

### Observations from fig 3.12(active camber vs active steering)

- Active camber stabilises the roll angle very rapidly without causing much fluctuations. However active steering also stabilises roll but only after some fluctuations
- At higher velocities for active camber the yaw increased very rapidly and stabilised after some time but yaw could not reach the zero value
- For active steering, even though yaw reached the zero value there were some fluctuations

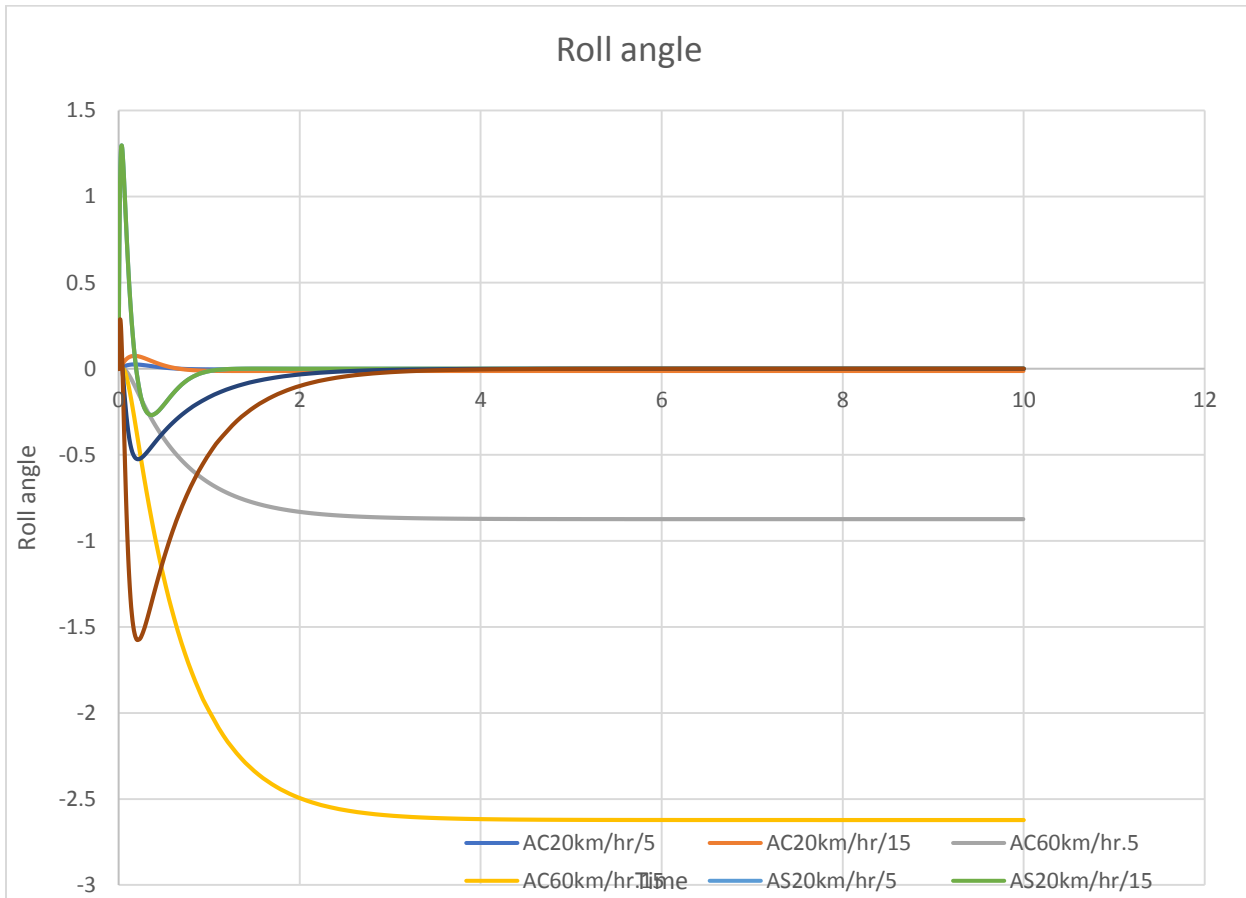


Fig 3.12: variation of roll during active camber vs active steer for desired yaw generated from equivalent 5° steering and 15° steering with .001 understeer coefficient at 20 and 60 kmph

## 4. CONCLUSION

The variations of different lateral parameters like lateral velocity, yaw and roll angle were compared and analyzed by carrying out different simulations with individual effects of camber and steering, combined camber-steering, active camber and active steering. From all the iterations carried it was evident that active camber yielded the best results for the considered lateral parameters. For steering only, all the outputs generated were high compared to the values generated during other conditions. Also, the outputs generated in this case was found to be oscillating.

For camber, all the output values reached their stable conditions through a smooth transition. The maximum values reached by the output were low compared to steering only condition. Since steering and camber had different influences on the parameters taken, it was a necessity to analyses their combined effects on the output. The next set of simulations were carried out under the combined influence of camber and steering. As it was expected the outputs reached their stable values smoothly even though some fluctuations were present. However, it was negligible unlike the as in the previous case. The results in this case were much better in comparison to the previous cases.

The next set of simulations were carried out to analyses the lateral parameters under active steering and active camber conditions. The effects of active steering were found to be more influential at lower velocities but at higher velocities active camber took control over the output. Stable output values were achieved by active camber quicker than active steering at all speeds. For active steering there were some sudden fall in output values at the beginning but rose quickly and achieved stable values. In case of active camber, the transition was smoother. It can be concluded that more detailed studies on the lateral parameters under the combined influence of active camber and active steer is of great potential in the field of vehicle dynamics.

# Reference

1. A.Carcaterra, VEHICLE SYSTEM DYNAMICS, Edition 2019-2020 –LECTURE NOTES
2. Manning WJ and Crolla DA. A review of yaw rate and sideslip controllers for passenger vehicles. *TI Meas Control* 2007; 29: 117–135.
3. Ataei M, Khajepour A and Jeon S. A General Rollover Index for Tripped and Un-tripped Rollovers on Flat and Sloped Roads. *Proc IMechE, Part D: J Automobile Engineering* 2017; 233: 304–316
4. Laws SM. An active camber concept for extreme maneuverability: mechatronic suspension design, tire modeling, and prototype development. *PhD Thesis, Stanford University, Stanford, CA*, 2010.
5. T. Yoshino and H. Nozaki, About the effect of camber control on vehicle dynamics, *SAE Technical Paper 2014-01-2383* (2014).
6. Daimler, The research vehicles of mercedes-benz, <http://www.daimler.com>, (2001).
7. A. Zachrisson, M. Rösth, J. Andersson, and R. Werndin, Evolve - a vehicle-based test platform for active rear axle camber and steering control, *SAE Technical Papers 2003-01-0581* (2003).
8. Y. Hirano, Integrated control of tire steering angle, camber angle and driving and braking torque for individual in-wheel-motor vehicle, *JSAE-SICE Benchmark Study for Automotive Control and Modeling*, No.3 (2012).
9. M. Horiguchi, A. Mizuno, M. Jones, and K. Futamura, Active camber control, *FISITA*, Vol. 198 LNEE (2013) pp. 247–256.
10. Matlab, [www.mathworks.com](http://www.mathworks.com)
11. B. Shyrokau, J. Loof, O. Stroosma, and M. Wang, Effect of steering model fidelity on subjective evaluation of truck steering feel, *Driving Simulation Conference, Germany* (2015).
12. R. Allen and T. Rosenthal, Requirements for vehicle dynamics simulation models, *SAE Technical Paper940175* (1994).
13. W. Bergman and D. Pelargus, The Role of Steer and Sideslip in the Mechanism of Slip Angle, *SAE Technical Paper, 960999*, 1996.
14. A. Hac and M. D. Simpson, Estimation of Vehicle Side Slip Angle and Yaw rate, *SAE Technical Paper, 2000-01-0696*, 2000.
15. D. Odenthal, T. Bunte, J. Ackermann, Nonlinear steering and Braking Control for Vehicle Rollover Avoidance, *European Control Conference, Karlsruhe, Germany*, 1999.

# Appendix

## Appendix A: MatLAB Code for Active camber and Active Steering System

```

cf=20000;
car = 20000;
ms = 680;
hs = 0.4;
u = 4.71;
Ix = 2100;
m = 800;
b = 1.25;
cp = 784;
a = 1.25;
Iz = 480;
kp = 11760;
g = 9.8;
Ca1 = 20000;
Ca2=20000;
Cg1 = 20000;
Cg2 = 20000;
Cg3 = 20000;
Cg4 = 20000;
g1=0.0872;
g2=0.0872;
g3=0.0872;
g4=0.0872;
d1=0.2;
d2=0.2;

```

```

Imh=(-ms^2*hs^2)/(Ix);
Ikh=(kp*ms*hs)/(Ix);
a11=(-(2*cf+car))/((m+Imh)*u);
a12= (-(Imh + m*u^2 + 2*a*cf-b*car))/((m+Imh)*u);
a13= (-Imh+Ikhanh)/(m+Imh);
a14=((cp*ms*hs)/Ix)/(m+Imh);
a21=(-(2*a*cf-b*car))/(u*Iz) ;
a22=(-(2*a^2*cf)+(b^2*car))/(u*Iz);
a23= 0;
a24=0;
a31=0;
a32=0;
a33=0;
a34=1;

```

```
a41=((2*cf*ms)+(car*ms*hs))/Ix)/((m+Imh)*u);
a42=((2*a*cf*ms)-(b*car*ms*hs))/Ix)/((m+Imh)*u);
a43=(-(m*kp)-(m*g*ms*hs))/Ix)/((m+Imh)*u);
a44=(-(m*cp)/Ix)/(m+Imh);
A= [a11 a12 a13 a14;a21 a22 a23 a24;a31 a32 a33 a34;a41 a42 a43 a44];
```

```
%b11=Ca1/(m+Imh);
%b12=Ca2/(m+Imh);
b13=Cg1/(m+Imh);
b14=Cg2/(m+Imh);
b15=Cg3/(m+Imh);
b16=Cg4/(m+Imh);
%b21=a*Ca1;
%b22=a*Ca1;
b23=a*Cg1;
b24=a*Cg2;
b25=-b*Cg3;
b26=-b*Cg4;
%b31=0;
%b32=0;
b33=0;
b34=0;
b35=0;
b36=0;
%b41=(-(ms*hs*Ca1))/(Ix*(m+Imh));
%b42=(-(ms*hs*Ca2))/(Ix*(m+Imh));
b43=(-(ms*hs*Cg1))/(Ix*(m+Imh));
b44=(-(ms*hs*Cg2))/(Ix*(m+Imh));
b45=(-(ms*hs*Cg3))/(Ix*(m+Imh));
b46=(-(ms*hs*Cg4))/(Ix*(m+Imh));
%B= [b11 b12 b13 b14 b15 b16; b21 b22 b23 b24 b25 b26; b31 b32 b33 b34 b35
b36;b41 b42 b43 b44 b45 b46];
B= [b13 b14 b15 b16; b23 b24 b25 b26; b33 b34 b35 b36; b43 b44 b45 b46];
```

```
C=eye(4);
D=zeros(4);
rank(ctrb(A,B))
if rank(ctrb(A,B))<4
    disp('Controlable')
else
    disp('Uncontrollable')
end

%Observability
```

```

rank(obsv(A,C))
if rank(obsv(A,C))<4
    disp('observable')
else
    disp('unobservable')
end

```

```

EigA=eig(A)
DetA=det(A)
ProdA=prod(eig(A))
SumA=sum(eig(A))
Q=eye(4)
R=10
K=lqr(A,B,Q,R)
%syms v r shy shy_dot
%X=[0.2 ;0.4 ;0.3 ;0.4];

%first transfer fuction
[num1,den1]=ss2tf(A,B,C,D,4)
sys1= tf(num1(1,1:5),den1)
pole(sys1)
bode(sys1,{0.001,100})

% 2nd transfer fuction
sys2= tf(num1(2,1:5),den1)
pole(sys2)
bode(sys2,{0.001,100})

% 3rd transfer fuction
sys3= tf(num1(3,1:5),den1)
pole(sys3)
bode(sys3,{0.001,100})

% 4th transfer fuction
sys4= tf(num1(4,1:5),den1)
pole(sys4)
bode(sys4,{0.001,1000})
bode(sys1,sys2,sys3,sys4)
linearSystemAnalyzer(sys1,sys2,sys3,sys4)

```

## Appendix B: Eigen Values and Stability

### Camber as input and influence of the system

All the real part of eigen values are negative and the system is asymptotically stable.

EigA = 4x1 complex

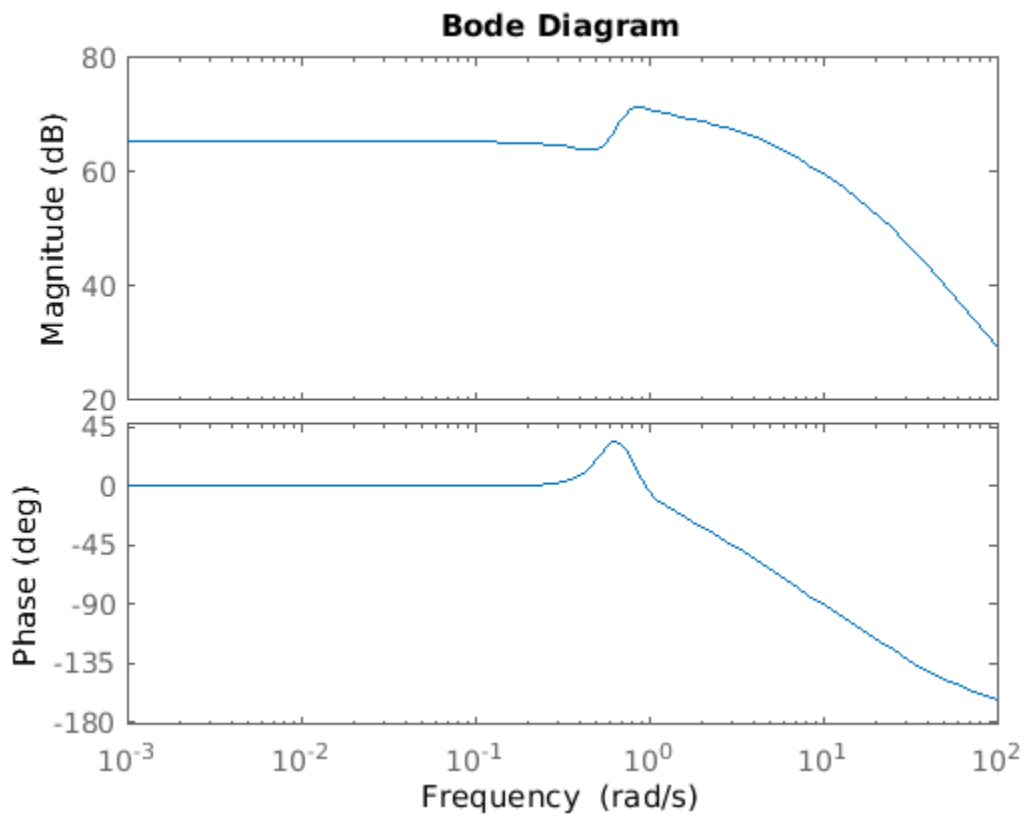
-26.7870 + 0.0000i

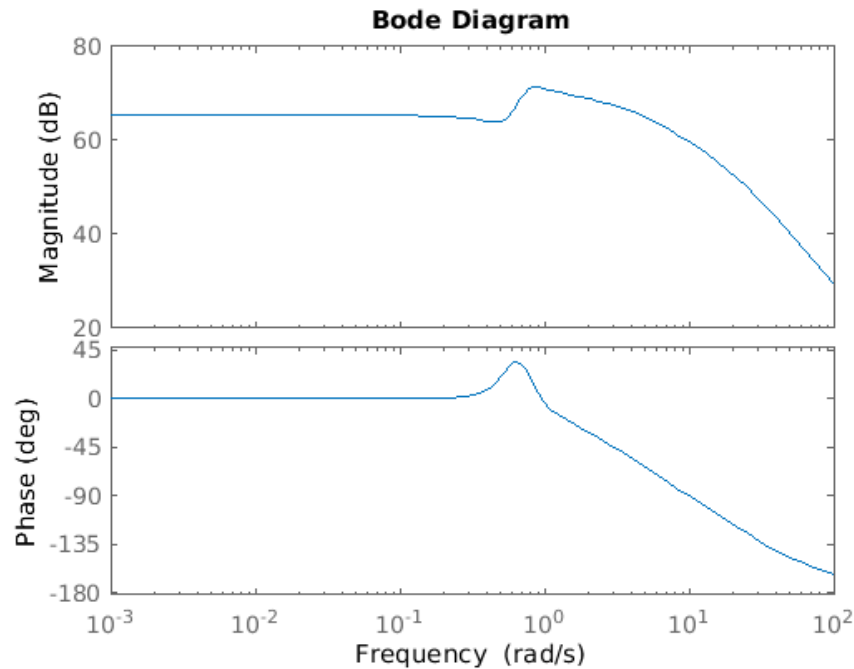
$$G(s) \frac{v}{\gamma_1 \gamma_2 \gamma_3 \gamma_4} = \frac{26.15s^3 + 2.968e05 s^2 + 1.04e05 s + 1.021e05}{s^4 + 30.87s^3 + 111.4s^2 + 56.58s + 54.79}$$

-3.6811 + 0.0000i

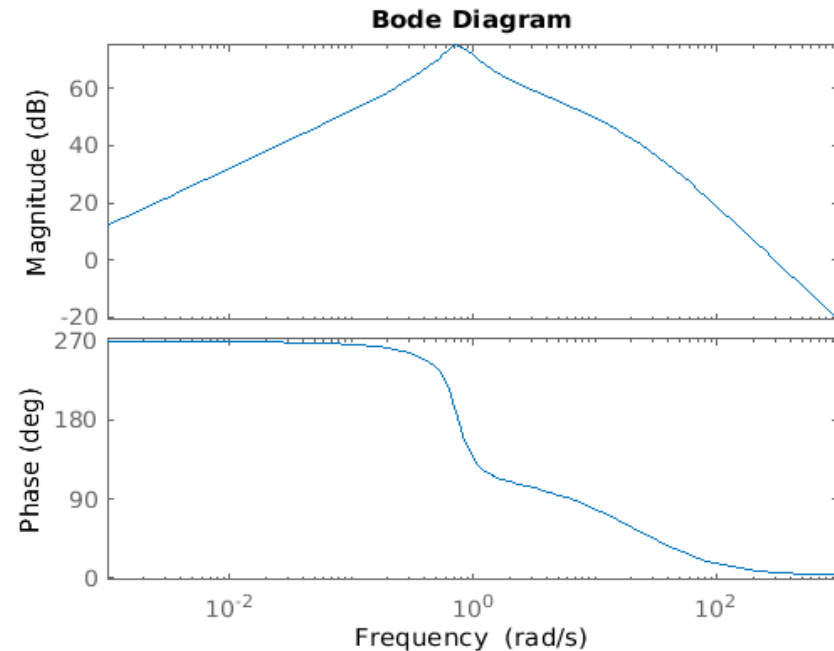
-0.2011 + 0.7178i

-0.2011 - 0.7178i





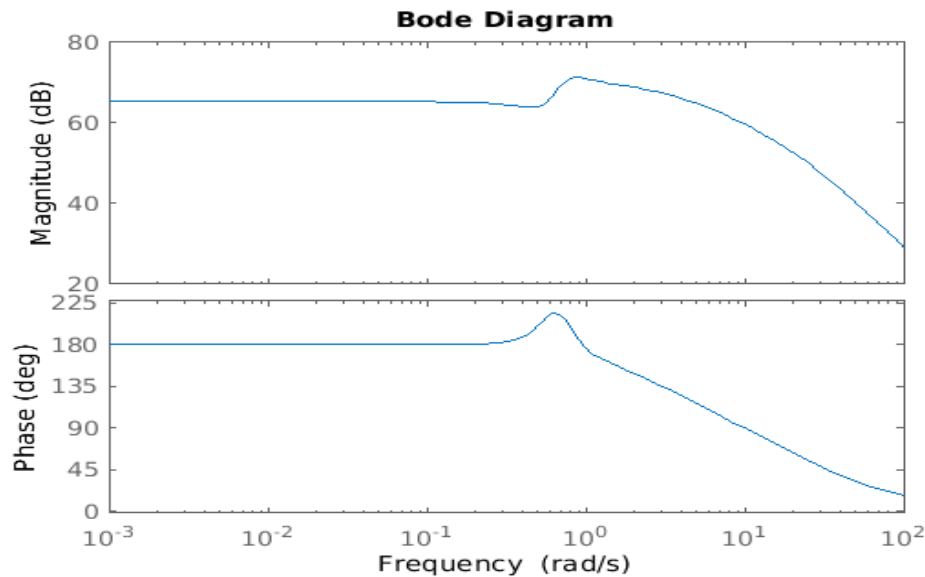
$$G(s2) \frac{r}{\gamma_1, \gamma_2, \gamma_3, \gamma_4} = \frac{-2.5e04S^3 - 4.265e05S^2 - 1.725e05S + 1.808e05}{S^4 + 30.87S^3 + 111.4S^2 + 56.58S + 54.79}$$



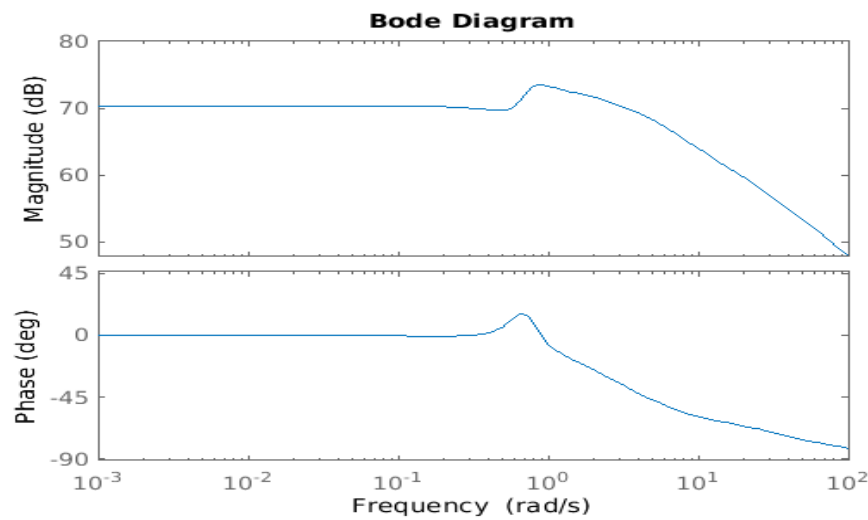
$$G(s4) \frac{\varphi}{\gamma_1, \gamma_2, \gamma_3, \gamma_4} = \frac{-3.387S^3 - 8.989e04 S^2 - 2.181e05 S + 3e-10}{S^4 + 30.87S^3 + 111.4S^2 + 56.58S + 54.79}$$

Continuous-time transfer function.

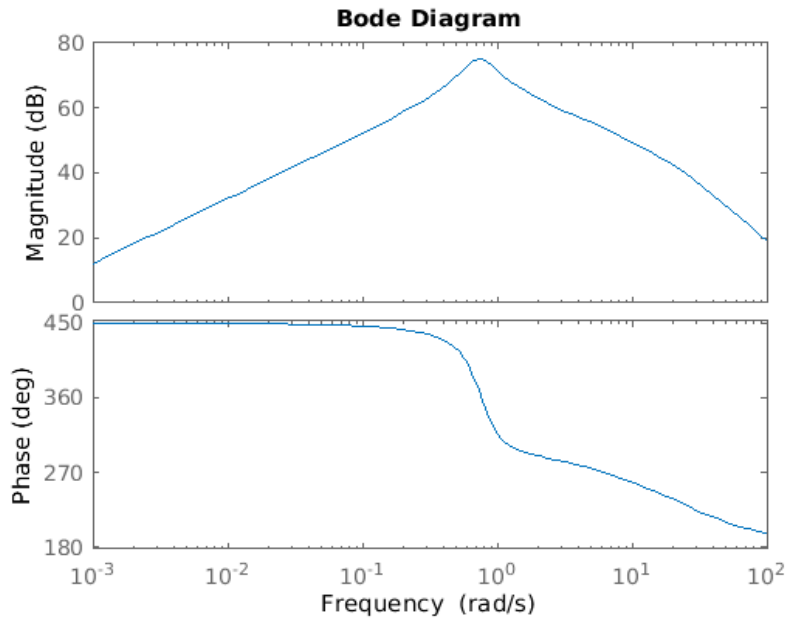
## Steering as input and influence of the system



$$G(s) \frac{v}{\delta_1, \delta_2} = \frac{26.15 S^3 - 2.961e05 S^2 - 1.037e05 S - 1.016e05}{S^4 + 30.87S^3 + 111.4 S^2 + 56.58S + 54.79}$$

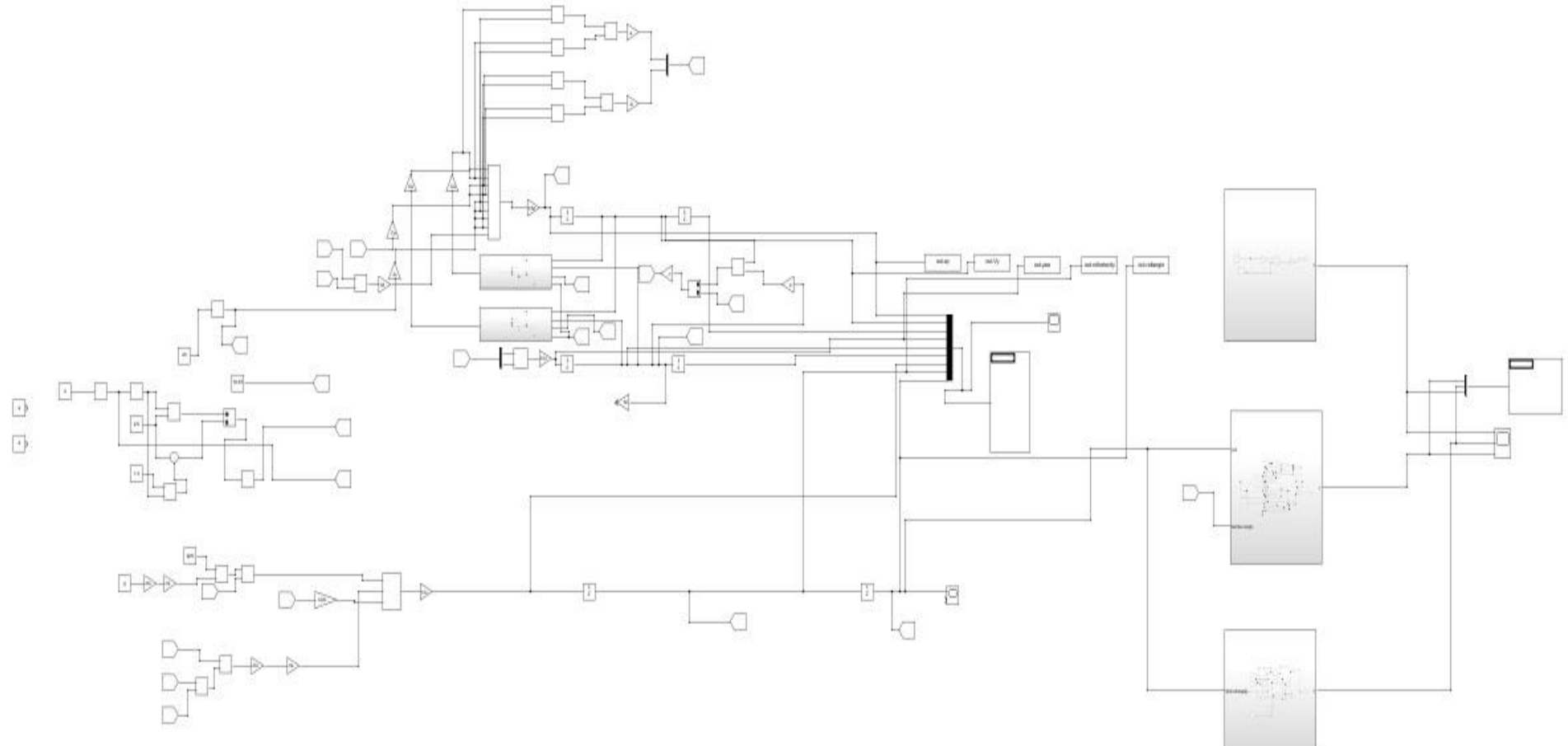


$$G(s2) \frac{r}{\delta_1, \delta_2} = \frac{2.5e04 S^3 + 4.259 e05 S^2 + 1.722 e05 S + 1.804e05}{S^4 + 30.87 S^3 + 111.4 S^2 + 56.58 S + 54.79}$$



$$G(s4) \frac{\varphi}{\delta_1, \delta_2} = \frac{-3.387 S^3 + 8.991 e04 S^2 + 2.184e05 S + 1.527e-10}{S^4 + 30.87 S^3 + 111.4 S^2 + 56.58 S + 54.79}$$

## Appendix C: Simulink Model





SAPIENZA  
UNIVERSITÀ DI ROMA